

CECW-ED  Engineer Technical Letter 1110-2-551	Department of the Army U.S. Army Corps of Engineers Washington, DC 20314-1000	ETL 1110-2-551  31 August 1998
	Engineering and Design  IDENTIFICATION, INSPECTION, AND EVALUATION OF FRACTURE CRITICAL MEMBERS OF IN-SERVICE BRIDGES	
	<b>Distribution Restriction Statement</b> Approved for public release; distribution is unlimited.	

CECW-ED

Technical Letter  
No. 1110-2-551

31 August 1998

**Engineering and Design  
IDENTIFICATION, INSPECTION, AND EVALUATION  
OF FRACTURE CRITICAL MEMBERS OF IN-SERVICE BRIDGES**

**1. Purpose**

This Engineer Technical Letter (ETL) provides guidance in the identification, inspection, and evaluation of fracture critical members of in-service bridges owned and operated by the U.S. Army Corps of Engineers (USACE) on Civil Works projects. This ETL is not intended to provide guidance on analysis and design of bridges.

**2. Applicability**

This ETL applies to all USACE Commands having responsibilities for planning, inspecting, evaluating, and documenting the safety of in-service bridges.

**3. References**

References are listed in Appendix A.

**4. Distribution Statement**

Approved for public release; distribution is unlimited.

**5. Background**

*a.* The national average for bridge failures per year is 150 collapses resulting in the death of 12 people. Nationally, bridge collapses are not now as frequent as they were in the nineteenth century; however, they still occur. It is extremely important that fracture critical members on

bridges be identified, properly inspected, and evaluated.

*b.* As noted in Appendix A, a significant amount of information is currently published on inspecting and evaluating fracture critical members. A methodology for identifying fracture critical members is explained in this ETL. Information pertaining to state-of-the-art techniques for real-time damage assessment of bridge structures is provided in Appendix B.

**6. Summary**

This ETL summarizes procedures for the identification, inspection, and evaluation of fracture critical members of USACE in-service bridges on public roads. The ETL is not intended to provide guidance on how to develop a numerical model, apply loads and boundary conditions, or develop load combinations. However, once a structural model has been developed, this ETL will provide guidance on identifying, inspecting, and evaluating fracture critical members of in-service bridges. Two bridges, Summit Inland Waterway Bridge crossing the Delaware River and Chesapeake Bay and St. George's Highway Bridge located in Delaware and Maryland crossing the Chesapeake Bay and Delaware Canal, are analyzed using the finite element method to demonstrate a procedure of locating fracture critical members. The structural degradation process resulting from fracture and fatigue is presented to provide background for critical assessment and inspection planning. A state-of-the-art review of new techniques in

structural damage monitoring and structural integrity assessment methodology is presented in Appendix B. This review summarizes information pertaining to new methodology and technology available for more effective inspection and evaluation of bridges. The reader should be aware that the information in Appendix B is new technology and may not apply to all conditions. CECW-ED should be contacted if there is a concern about applicability.

### **7. Objectives**

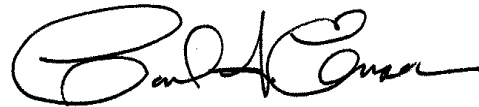
The objective of this ETL is to provide information on the identification, inspection, and

FOR THE COMMANDER:

evaluation of fracture critical members on in-service bridges. In addition, this ETL provides information pertaining to state-of-the-art review of new techniques for real-time damage assessment of bridge structures.

### **8. Action**

The guidance in this ETL should be used to identify, inspect, and evaluate fracture critical members on bridges owned and operated by USACE on Civil Works projects.



CARL F. ENSON, P.E.  
Chief, Engineering Division  
Directorate of Civil Works

CECW-ED

Technical Letter  
 No. 1110-2-551

31 August 1998

**Engineering and Design  
 IDENTIFICATION, INSPECTION, AND EVALUATION  
 OF FRACTURE CRITICAL MEMBERS OF IN-SERVICE BRIDGES**

**Table of Contents**

Subject	Paragraph	Page	Subject	Paragraph	Page
<b>Chapter 1</b>			Fracture Analysis Procedure . . . . .	4-3	4-1
<b>Introduction</b>			Fatigue Analysis Procedure . . . . .	4-4	4-6
Overview . . . . .	1-1	1-1	Prediction of Crack Growth . . . . .	4-5	4-11
Organization . . . . .	1-2	1-1	Fracture and Fatigue Assessment		
			Procedures . . . . .	4-6	4-12
			Development of Inspection Schedule	4-7	4-13
			Fitness-for-Service Assessment		
			Procedure . . . . .	4-8	4-13
<b>Chapter 2</b>			<b>Chapter 5</b>		
<b>Locating Fracture Critical Members</b>			<b>Conclusion</b>		
Fracture Critical Members . . . . .	2-1	2-1			
Analysis Procedure for Locating FCMs			<b>Appendix A</b>		
of Non-Truss Bridges . . . . .	2-2	2-2	<b>References</b>		
Analysis Procedure for Locating FCMs					
of Truss Bridges . . . . .	2-3	2-2	<b>Appendix B</b>		
Guidance for Locating FCMs . . . . .	2-4	2-7	<b>A Review of State-of-the-Art</b>		
			<b>Techniques for Real-Time</b>		
			<b>Damage Assessment of Bridges</b>		
<b>Chapter 3</b>					
<b>Inspection Planning and Quality</b>					
<b>Control of Fracture Critical Members</b>					
Overview . . . . .	3-1	3-1			
Inspection Planning and Quality					
Control . . . . .	3-2	3-1			
NDT and Evaluation . . . . .	3-3	3-1			
Guidance for Field Inspection . . . . .	3-4	3-2			
<b>Chapter 4</b>					
<b>Engineering Critical Assessment</b>					
<b>Procedures</b>					
Overview . . . . .	4-1	4-1			
Fracture Behavior of Steels . . . . .	4-2	4-1			

## Chapter 1 Introduction

### 1-1. Overview

*a.* As of November 1991, 35 percent of approximately 590,000 bridges in the United States were considered structurally deficient or functionally obsolete (Bagdasarian 1994). Many bridges have become deficient due to aging and heavier than expected service loads. In particular, some highway and railroad bridges ranging from 50 to more than 100 years old are still performing their intended functions in spite of excessive use (Scalzi 1988). The recent collapse or near-collapse of some bridges has resulted in the development of extensive inspection programs and engineering assessment methods to ensure that highway bridges are safe for public use.

*b.* Highway bridges are subjected to a wide range of vehicular loads. As vehicles cross, the live loads produce changing stresses which cause a wide range of strain or deformation in the members. The impact of a vehicle also contributes to the changing stresses. The relatively large range of repeated elastic strain or deformation places greater demands on the material properties of critical members and increases the probability of damage. In addition, bridges are relatively unprotected from the environment. Bridge members are exposed to water, debris, and contaminants such as deicing salts, and they must resist freeze/thaw damage and accommodate significant thermal movement.

*c.* Bridge deterioration typically occurs at specific locations related to deck drainage, debris accumulation, and exposure. Cracks can initiate at stress concentrations caused by certain framing details and fabrication defects. To evaluate the degree to which a deficiency effects safety often requires an appraisal of that specific deficiency's significance on the structural stability of the bridge. Locating the fracture critical members of

the bridge, as well as assessing the criticality of deficiencies in the fracture critical members (FCMs), is necessary to determine if the bridge should remain open. An effective inspection plan must contain information helpful in locating problems on members with potentially high-risk modes of failure. Unless the inspector understands where to look and what to look for when inspecting bridges, the inspection activity will be ineffective. Cracks frequently start at stress concentrations and out-of-place stresses due to connections of transverse members. Additional information on structural inspection can be found in Chapter 2 of the AASHTO (1983) Manual for Maintenance Inspection of Bridges, and Chapter 18 of the FHWA (1991) Bridge Inspector's Training Manual 90.

### 1-2. Organization

This report summarizes the procedures for identification, inspection, and evaluation of FCMs of USACE in-service bridges on public roads. In Chapter 2, two bridges that cross the Chesapeake Bay to the Delaware River canal, Summit Inland Waterway Bridge and St. George's Highway Bridge, are analyzed using the finite element method to demonstrate a procedure of identifying FCMs. In Chapter 3, the structural degradation process due to fracture and fatigue is presented to provide background for critical assessment and inspection planning. A review of state-of-the-art techniques in structural damage monitoring and structural integrity assessment methodology is presented in Appendix B. This review summarizes information pertaining to new methodology and technology available for more effective inspection and evaluation of bridges. This report is not intended as a stand-alone technical resource on fracture critical members. However, several references are included to provide the reader with additional information. Information provided in this report and other referenced documents is in a mixture of SI metric units and inch kip units. A more consistent set of equations will be developed in a future Engineer Manual.

## Chapter 2 Locating Fracture Critical Members

### 2-1. Fracture Critical Members

*a.* The AASHTO (1996) Guide Specification for Fracture Critical Bridge Members states that “Fracture Critical Members or member components are tension members or tension components of members whose failure would be expected to result in collapse of the bridge.” To qualify as a FCM, the member must be a nonredundant member subject to tensile force. There must not be any other member or system of members which will serve the functions of the member in question should it fail. This has also been interpreted to include bending members which experience tensile forces over part of their cross section, whose failure would be expected to result in collapse of the bridge. Compression members or components are not considered fracture critical. Since it is considered undesirable from an operation and maintenance standpoint to have a bridge member yield, collapse is taken to mean yielding has occurred. This is consistent with the approach used by the Federal Highway Administration. The FCM can be identified by removing the member in tension and checking the remaining members in the bridge to see if any members have yielded. Information on redundancy in bridge framing systems and of tension members, along with the necessary definitions, are included in Chapter 2 of the Federal

Highway Administration’s “Bridge Inspector’s Training Manual 90” (Hartle et al. 1991). In addition, pertinent articles on FCMs have been published in Civil Engineering (1987).

*b.* To locate the FCMs in a bridge, both dead and live loads must be considered in the structural analysis. As defined by AASHTO Standard Specifications for Highway Bridges (1996), dead loads are the weight of the complete structure, including the roadway, sidewalks, car tracks, pipes, conduits, cable, and other public utility services. Dead loads do not change with time and need to be considered as permanent loads acting on the structure. Live loads consist of the weight of applied moving loads such as vehicles and pedestrians. Live loading on the roadway of bridges or incidental structure shall consist of standard trucks or lane loads which are equivalent to truck trains. Two systems of loading, the H loading and the HS loading, are defined by AASHTO specifications (1996). Standard truck loads, wheel spacing, weight distributions, and clearances for standard H and HS truck loading can be obtained from the specification. H20-44 and HS20-44 standard truck loads that will be applied in the examples discussed later in this section are shown in Figure 2-1.

*c.* The lane loads consist of uniform load per linear foot of traffic lane combined with a single concentrated load (or two concentrated loads in the case of continuous spans) so placed on the span as to produce maximum stress. The

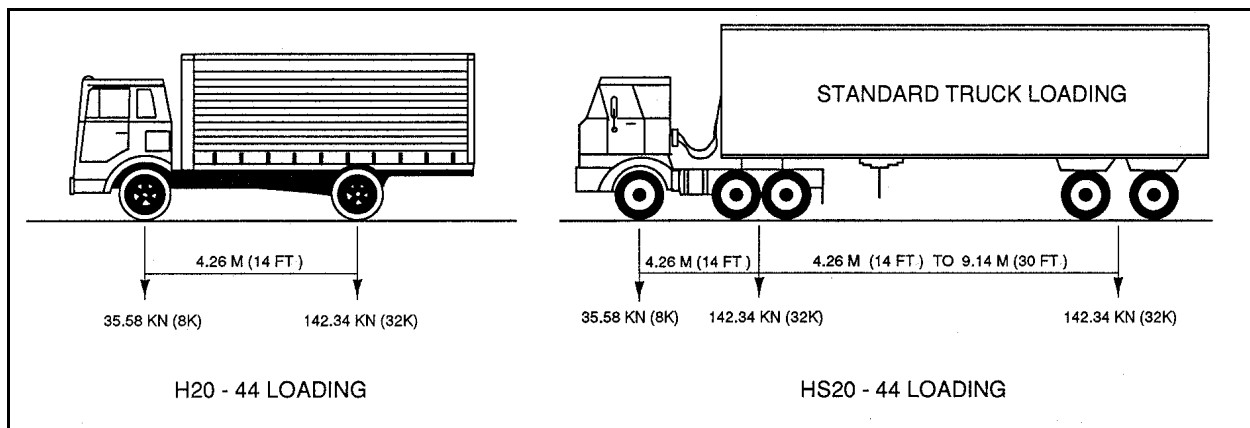


Figure 2-1. Standard truck loading

concentrated load and uniform load shall be considered as uniformly distributed over a 3-m (10-ft) width on a line normal to the center line of the lane. Figure 2-2 shows the lane loading for H20-44 and HS20-44. For the computation of moments and shears, different concentrated loads shall be used as indicated in Figure 2-2.

*d.* For continuous spans, the lane loading shown in Figure 2-2 needs to be modified by the addition of a second equal-weight concentrated load placed in one other span in the series in such position as to produce the maximum negative moment. Live load stresses produced by H or HS loading shall be increased for bridge superstructures and the portion of concrete or steel piles above the groundline which are rigidly connected to the superstructure as in rigid frames or continuous designs to account for impact effects. The amount of this allowance or increment should be calculated in accordance with AASHTO design specifications (1996).

## **2-2. Analysis Procedure for Locating FCMs of Non-Truss Bridges**

*a.* Figure 2-3 shows flowcharts for locating FCMs in non-truss bridges. Dead loads and live loads must be applied to the bridge according to AASHTO requirements. A structural analysis is

performed to determine the member forces. To locate FCMs, each tension member is removed on an individual basis to determine if its removal and the redistribution of forces cause any of the remaining members to yield. If yielding develops, the removed tension member is a FCM. The tested tension member is then reinstalled; the next tension member is removed, and the remaining members are again checked for yielding. This tension removal procedure continues until each tension member has been individually removed and the remaining members have been checked for yielding. After each tension member has been checked, a new live load condition is applied, and the tension member testing procedure is repeated. The FCMs for the entire bridge can be obtained utilizing this process.

*b.* Because this repeated analysis procedure can be very tedious and time consuming, the structural analysis can be performed by using a finite element structural program. ANSYS program (ANSYS 1992) is used for the example cases presented in paragraph 2-3.

## **2-3. Analysis Procedure for Locating FCMs of Truss Bridges**

*a.* For truss bridges, the first step of the analysis is to decide the degree of indeterminacy. For a

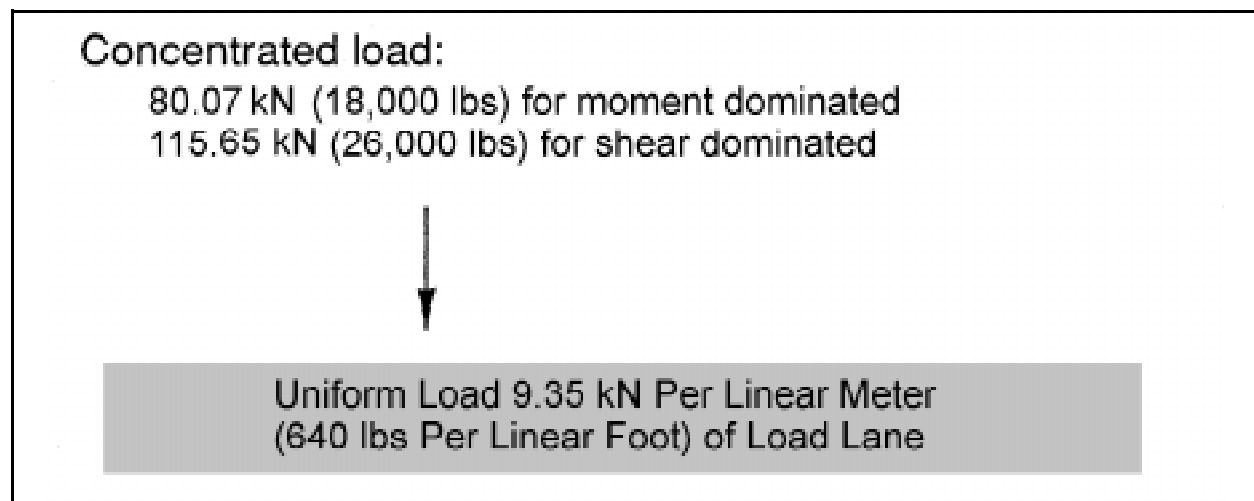


**Figure 2-2. H20-44 lane loading and HS20-44 lane loading**

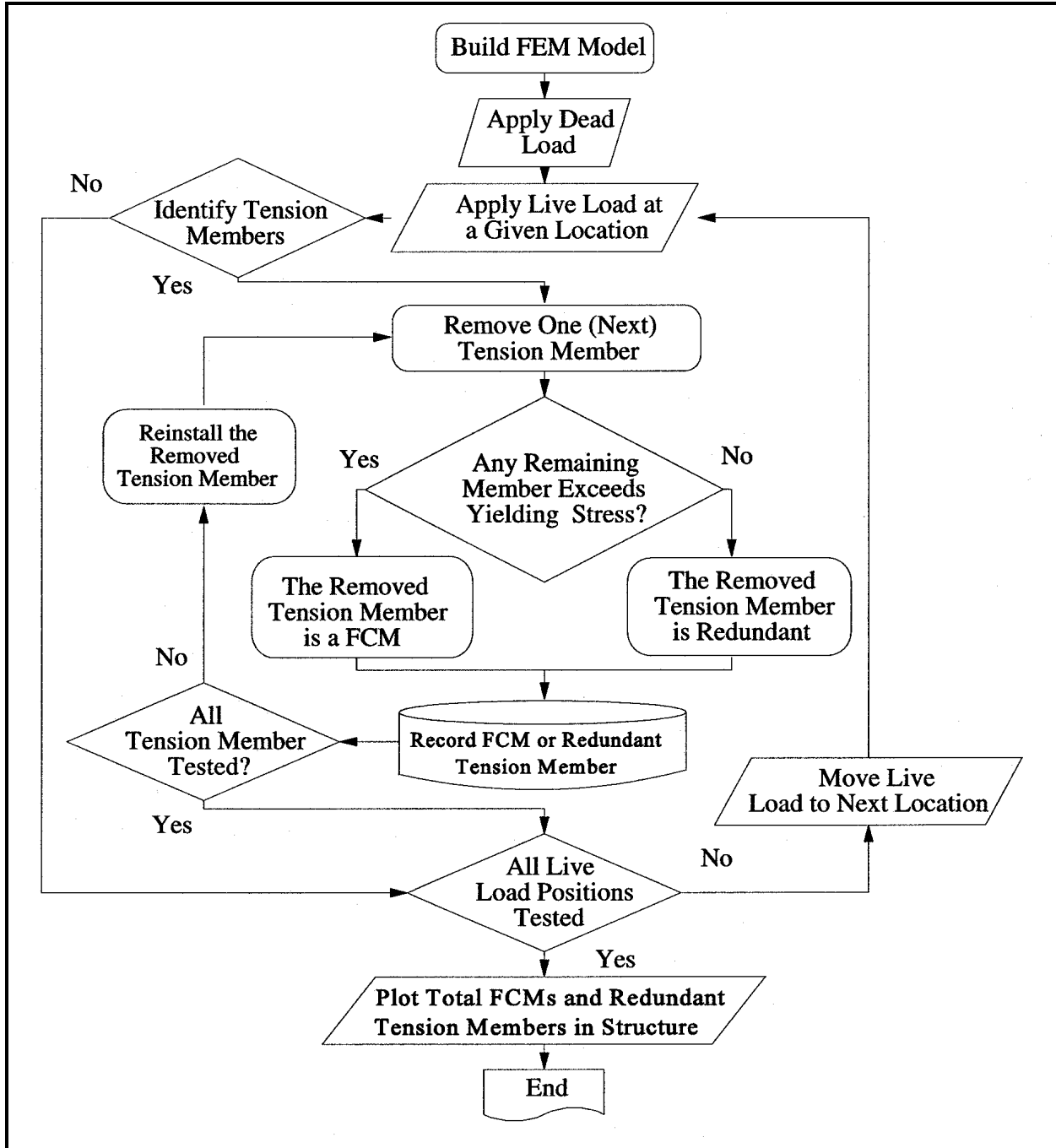


Figure 2-3. Flowchart for locating FCMs of non-truss bridges and indeterminate truss bridges using linear elastic and perfectly plastic model

determinate truss bridge all tension members are FCMs. The flowchart for determining FCMs of determinate truss bridges is presented in Figure 2-4. For an indeterminate truss bridge, the procedure is similar to a non-truss bridge as plotted in the flowchart in Figure 2-3.

b. Example 1 is Summit Bridge, an inland waterway bridge (627.28 m (2,058 ft) total span) crossing the Delaware River and the Chesapeake Bay. The bridge approach is via several simple supported girders, followed by a 76.2-m (250-ft) single-span deck truss (Figure 2-5), and then onto

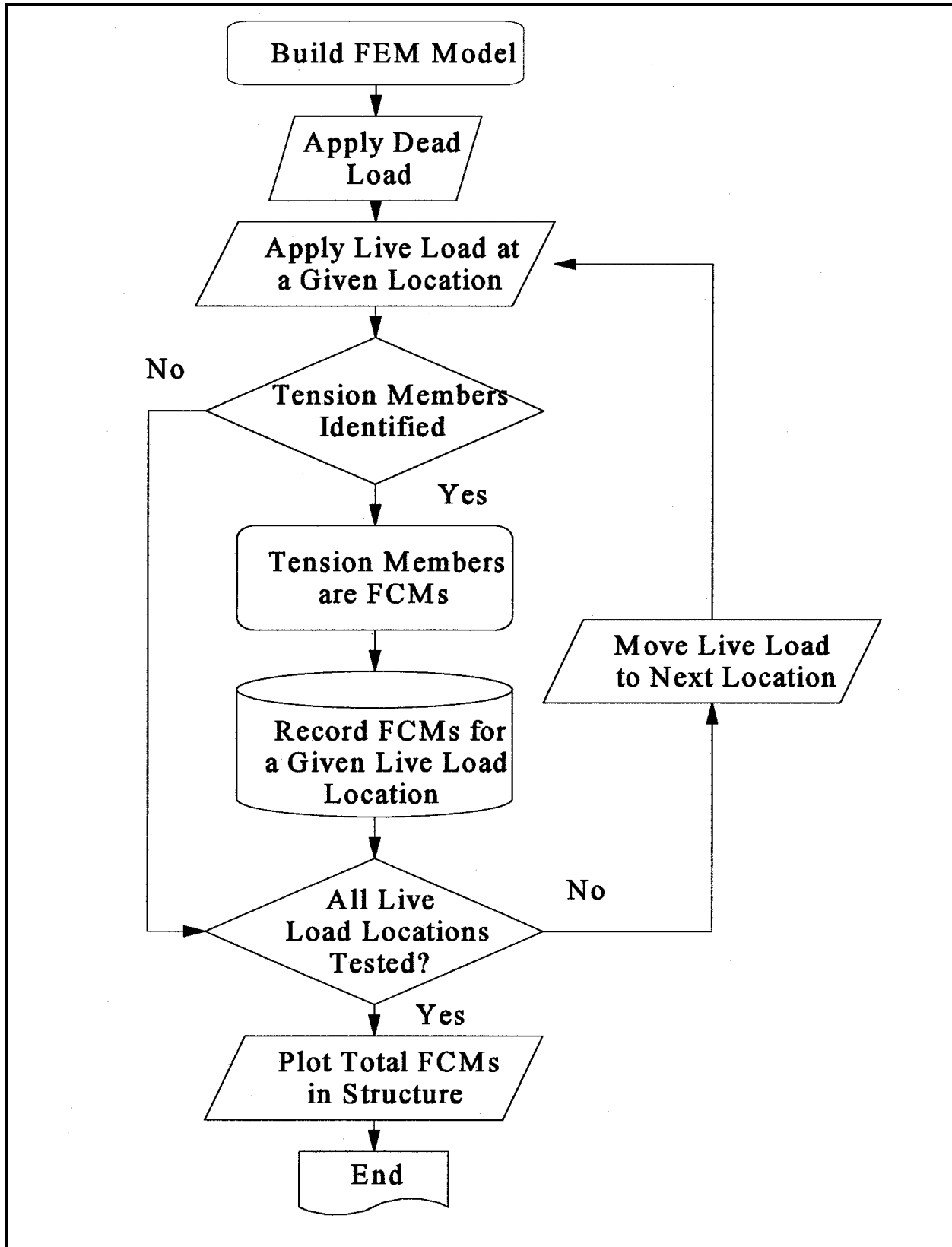


Figure 2-4. Flowchart for locating FCMs of statically determinate truss bridges

the 91.44-m (300-ft) anchor arm span and 182.88-m (600-ft) main span (Figure 2-6). The main span in the middle of the bridge (Figure 2-6) can be further divided into a suspended span and two cantilever spans. Figure 2-5 shows the finite element model of the deck truss. The deck truss system is a determinant (nonredundant) structure. Figure 2-6 shows the finite element model of the anchor arm and main spans. This bridge has four

traffic lanes. The dead loads of each bridge member were applied according to the design data (USACE 1940). The design live load is a HS20-44 loading (Figure 2-2) plus an impact load of 111.2 kN (25 kips) (USACE 1940), except for the deck slab which is designed for 142.34 kN (32 kips) per axle load. The 9.35 kN per linear meter (640 lb per linear foot) of lane load was applied as a distributed load to the truss

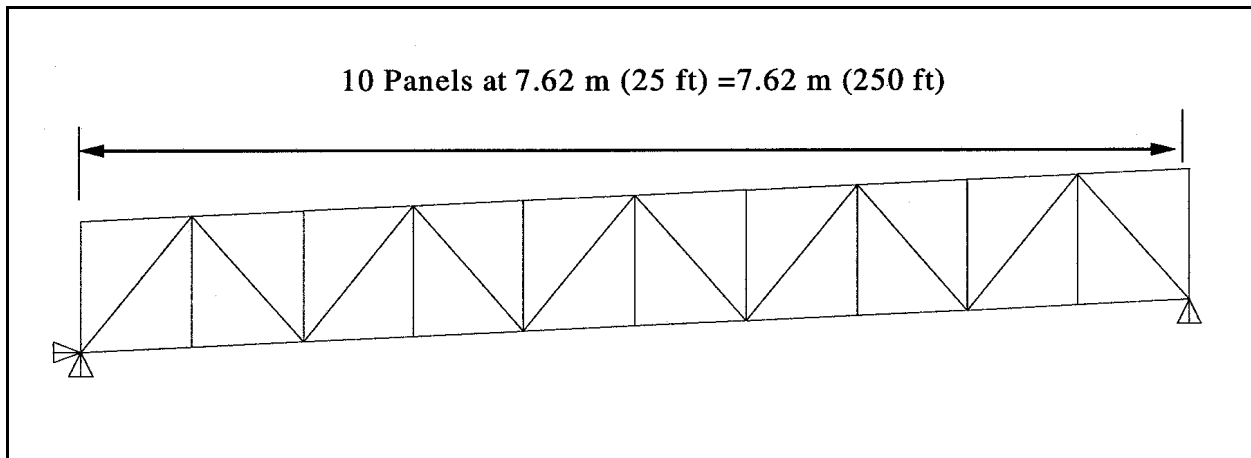


Figure 2-5. Summit Bridge (single-span deck truss)

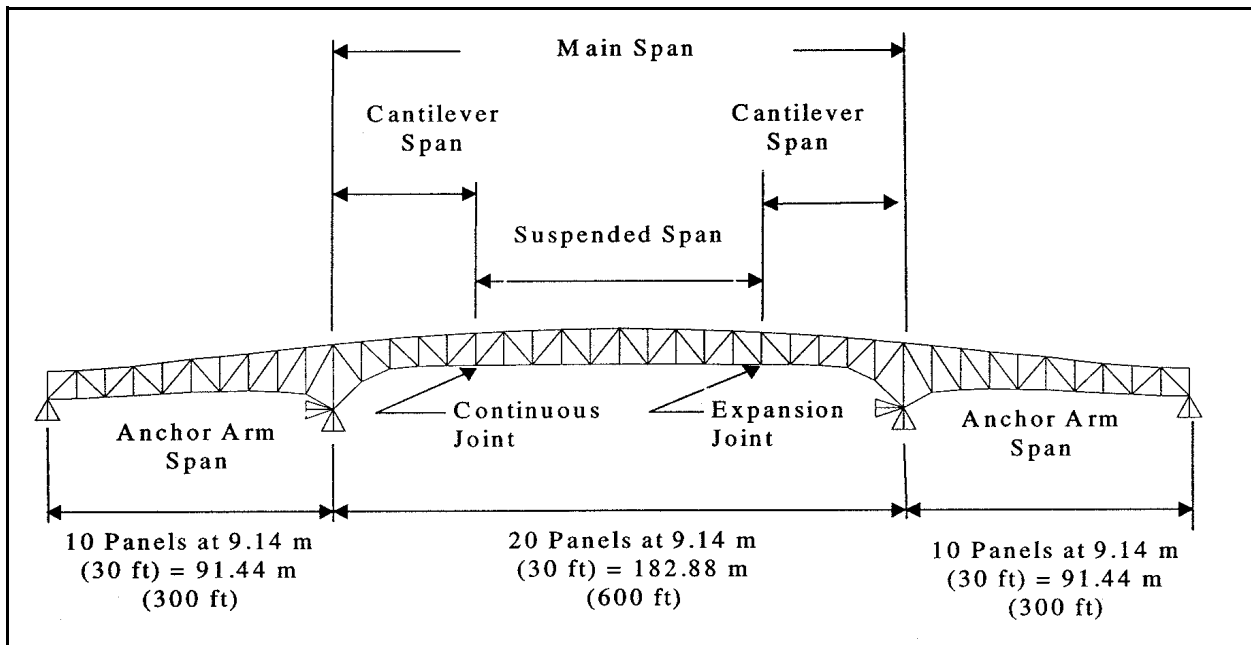


Figure 2-6. Summit Bridge (mid spans)

joints connected to the bridge deck. A concentrated live load of 115.65 kN (26 kips) plus the (111.2-kN (25-kip)) impact load were positioned at one truss joint connecting to the deck and were moved from one end of the bridge to the other end; then, the tension members were recorded. Since this is a determinate bridge, all the tension members recorded are FCMs. The results are shown in Figures 2-7 and 2-8.

c. Example 2 is St. George's Highway bridge, a tied-arch single span (164.59 m (540 ft)) bridge located in Delaware and Maryland crossing the Chesapeake and Delaware Canal. Since this bridge is not a truss bridge, Equation 2-1 does not apply. The finite element model is shown in Figure 2-9. St. George's Highway bridge is designed for H20-44 standard loading. As used for the Summit Bridge analysis, the same lane loading

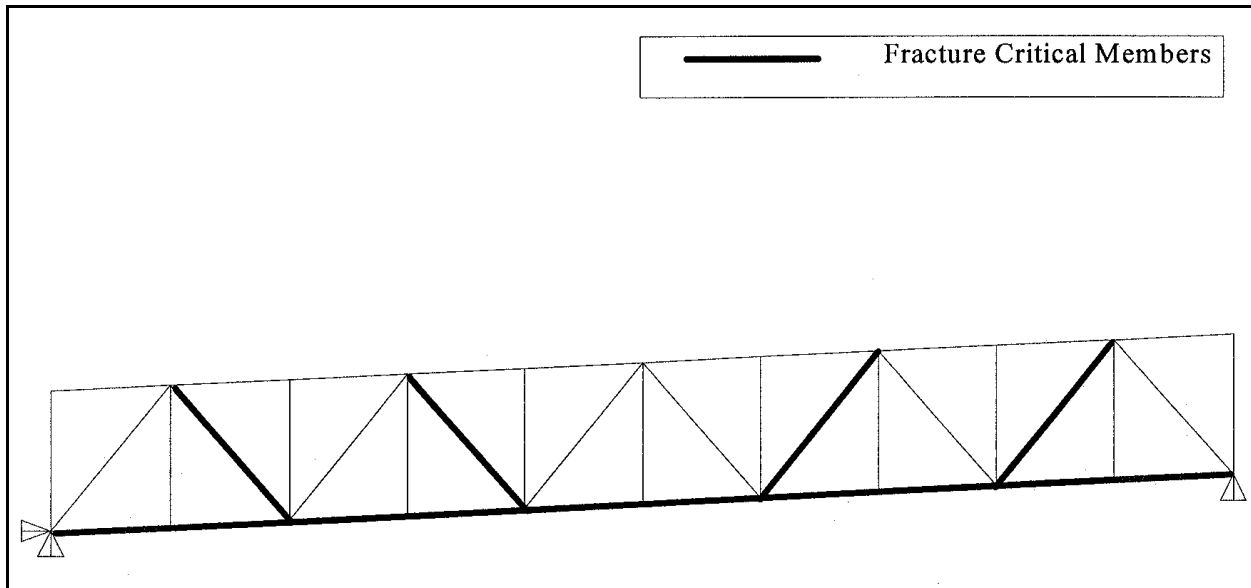


Figure 2-7. Summit Bridge (FCM in the simple span)

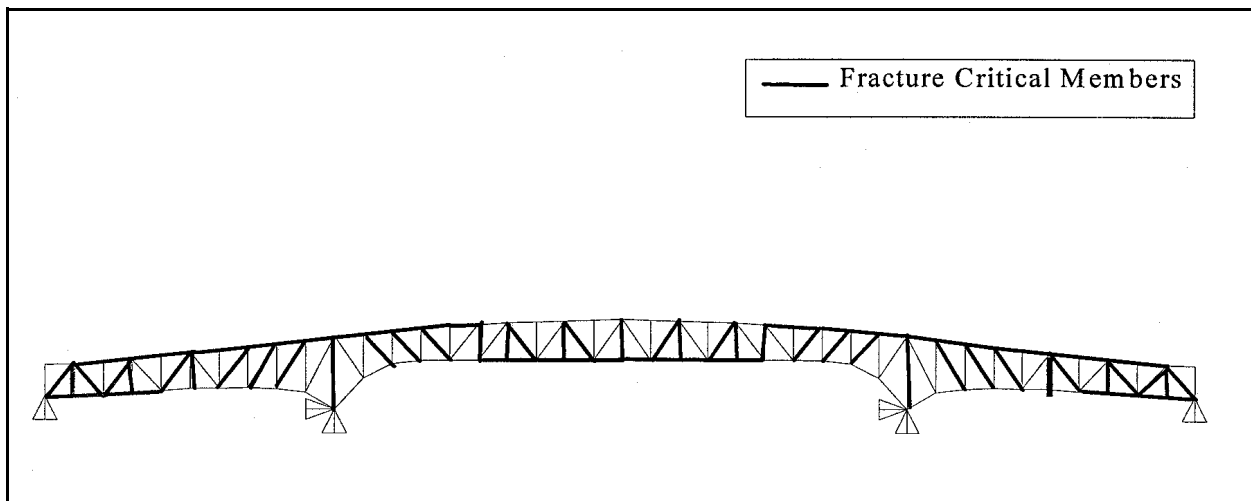
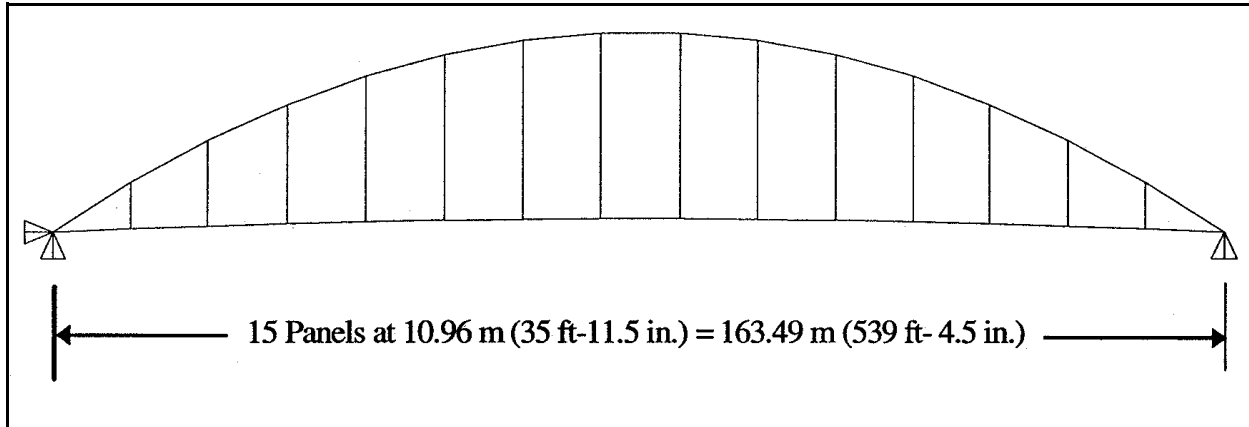


Figure 2-8. Summit Bridge (FCM in the mid spans)



**Figure 2-9. St. George's Highway Bridge (tied arch span)**

(HS20-44) was applied to this bridge. After the dead loads were applied to each bridge member and the concentrated load was moved to all the deck joints, the tension members were identified (USACE 1956). For a concentrated loading position, each tension member was individually removed to determine if the redistribution of the load caused any remaining members to reach yield stress. If yielding occurred in the remaining members, the tension member removed was considered to be a FCM. If yielding did not occur, the removed tension member was considered a redundant member. The concentrated live load was then moved to the next deck joint. The process was repeated until all the FCMs were identified. The FCMs for the St. George's Highway Bridge are shown in Figure 2-10.

#### **2-4. Guidance for Locating FCMs**

*a.* From the results shown for the simple-span deck truss, it can be observed that the bottom chord must be composed of tension members because it stretches as the span bends. The diagonal truss members may be in tension or compression. Harland et al. (1986) proposed that, for controlling loads uniformly distributed across the span length, diagonals pointing upward towards the truss mid-span are subject to compression, while diagonals pointing upward away from the mid-span are subject to tension. The results from the Summit Bridge analysis shown in Figure 2-7 support Harland's proposition.

*b.* From the results shown in Figure 2-8, the top chord is in tension in the area over the piers. In the area near the end support (abutment), the truss is similar to the simple spans; therefore, the bottom chord is in tension. However, when using visual inspection of the framing arrangement, there are transient zones in which it is not obvious if the members are in tension or compression. The FCMs in these zones become obvious by analysis using the procedure outlined in Figure 2-3.

*c.* The suspended span for Summit Bridge acts as a simple span; therefore, the same principles as noted in paragraph 2-4a above apply as shown in Figure 2-8.

*d.* The tied-girder prevents the separation of supports; therefore, it is in tension. Any fracture in the girder will cause partial or total collapse of the bridge; therefore, the tied girder is a FCM. The members suspended from the arch are also subject to tension; however, they must be investigated to see if the failure of one suspension member could cause the remaining members to yield.

*e.* The guidelines set forth in this ETL can help bridge engineers to generally locate FCMs using visual observation. However, it is suggested that the procedures shown in Figures 2-3 and 2-4 be used to specifically identify the FCMs. FCMs should be identified during initial bridge design and documented as part of the permanent design file.

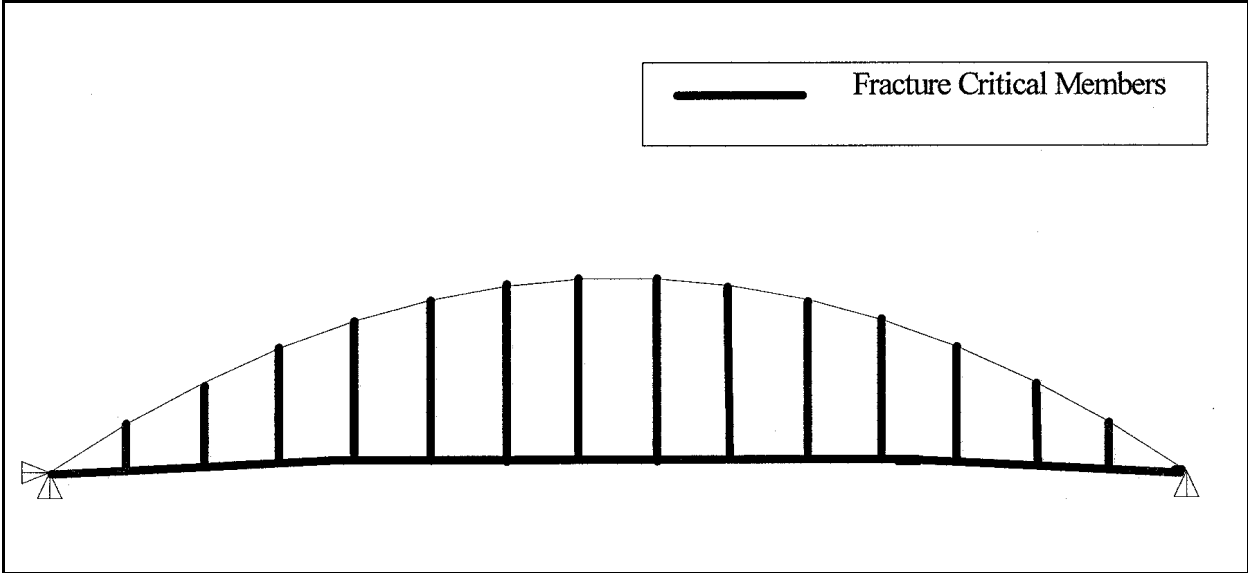


Figure 2-10. St. George's Highway Bridge (FCM in the tied arch span)

## Chapter 3 Inspection Planning and Quality Control of Fracture Critical Members

### 3-1. Overview

The inspection of FCMs should receive the highest priority in any bridge inspection program. Some FCMs may have details that are highly susceptible to damage due to repeated loading (i.e., fatigue), or others may be in poor condition due to corrosion or damage. Repairs and modifications can influence the likelihood of problems. The inspector should recognize that age and heavy traffic, particularly trucks, can compound problems. Inspection planning should consider the age of the bridge and traffic information if available.

### 3-2. Inspection Planning and Quality Control

*a.* Inspection planning involves having the appropriate equipment available to permit a hands-on inspection. Factors such as location, capacity, traffic, roadway width, height, and water depth must be considered in selecting access equipment. The special equipment may also require more elaborate traffic control provisions or staging.

*b.* The level of inspection should be tailored appropriately for the bridge being inspected. When establishing priorities for bridge inspection, consideration should be given to the age of the bridge, number of cycles since last inspection, fatigue category for connections and attachments, and extent of nondestructive testing (NDT) during the original fabrication and subsequent repairs. The bridges should be categorized and ranked in order of criticality so that the resources available for the inspections are used to provide the highest degree of safety.

(1) If it becomes necessary to establish bridge inspection priorities, a structural engineer with experience in both load rating and evaluating the

types of bridges being considered should be involved in the process. Several things influence relative criticality:

- (a) The degree of redundancy.
  - (b) The live load member stress.
  - (c) The propensity of the material to crack or fracture.
  - (d) The condition of specific FCMs.
  - (e) The existence of fatigue-prone design details.
  - (f) The previous and predicted number and size of loads.
- (2) Stress analysis using the finite element method, coupled with fracture mechanics analysis and materials testing may have to be pursued to identify the structural criticality if such condition is not easily determined.

### 3-3. NDT and Evaluation

*a.* There are a number of NDT methods available for quantifying the distressed condition of a FCM. No single test will meet all the needs for a given circumstance, and in many cases it will be necessary to use one or more of these tests in conjunction with another. When NDT is required, the testing must be performed by a person fully qualified in its use (e.g., ASNT Certified inspector). NDT can be conducted using the appropriate process and procedure applicable to the specific conditions being evaluated. The NDT processes commonly used for bridge inspection include visual testing (VT), dye penetrant testing (PT), magnetic particle testing (MT), and ultrasonic testing (UT). Radiographic testing (RT) and eddy current testing (ET) are not common for field applications. These test processes and procedures are covered in detail in American Welding Society (AWS 1985).

*b.* Serious problems discovered in FCMs must be addressed immediately. This should

include closing the bridge if the condition warrants. Less serious problems may require repair, retrofit, or partial closure of the bridge. The inspection results may find that the distress condition of a FCM is subcritical. However, problems may develop slowly over a period of time. The subcritical cracks may grow to a critical length (as discussed in Chapter 4), at which time catastrophic structural failure may occur suddenly. Therefore, periodic inspections and evaluations of FCMs are directed at determining the overall condition of the bridge and identifying potential problem areas before they reach a critical level. To ensure bridge safety, it is important that periodic inspections be performed to ensure that cracks are detected before reaching critical size. Periodic inspections should correlate with expected crack growth rates.

### **3-4. Guidance for Field Inspection**

*a.* In general, field inspections can be divided into two stages, a scheduled visual inspection and

a detailed inspection for structural evaluations. Distressed FCMs or an open surface crack length at least twice the joint thickness can usually be detected by visual inspection without using a magnifying glass or removing the surface coating. Intervals for scheduled visual inspections are in accordance with ER 1110-2-111.

*b.* If distress indications are found in FCMs by initial VT inspection, detailed inspections must be performed. Paint, corrosive oxides, dirt, debris, grease, and other surface materials on the member must be removed before more detailed PT, MT, or UT inspections can be scheduled to determine additional information pertaining to the conditions of the distress members. A fracture and fatigue analysis can also be performed at this stage to help evaluate how fit the bridge is for service.

*c.* Retrofitting or replacement of the distressed FCMs must be scheduled immediately if the analysis results indicate bridge failure is imminent.

## Chapter 4 Engineering Critical Assessment Procedures

### 4-1. Overview

When inspections reveal cracks, it is necessary to establish acceptance levels to determine if immediate repairs are needed to prevent fracture. The critical crack size may be determined through a fracture mechanic's evaluation for a given set of loads, environmental factors, geometry, and material properties. If the crack size is less than the critical dimension, the expected remaining life and rate of crack propagation may be determined by a fatigue analysis. The engineering decision on appropriate repair or planned maintenance is based on the concept of fitness-for-service of the distressed bridge (International Institute of Welding 1990). These analysis procedures are called Engineering Critical Assessment (ECA) procedures.

### 4-2. Fracture Behavior of Steels

*a.* The service temperature under which a steel bridge operates has a significant effect on the fracture behavior of the steel. The critical fracture stress remains unchanged by temperature for a given crack size if the service temperature is below a transition temperature, called nil ductility transition temperature. The critical stress decreases as the crack size increases and is inversely proportional to the square root of the crack size. Above the transition temperature, fracture stress of steels becomes less dependent on the crack size. As the material temperature increases, the fracture stress eventually reaches the yield strength, and then the ultimate strength, regardless of the crack size.

*b.* As the service temperature decreases, for low and intermediate strength steels, the material changes from ductile fracture behavior to brittle fracture behavior at the nil ductility transition temperature. Considering constraint, the appropriate fracture parameter,  $K_{Ic}$  (critical stress intensity

factor under plane strain condition) or crack tip opening displacement (CTOD) can be selected for evaluating the fracture behavior of the bridge material. Those fracture parameters are defined and discussed in detail by Barsom and Rolfe (1987).

### 4-3. Fracture Analysis Procedure

*a.* For bridges containing cracks and operating below the nil ductility transition temperature, linear elastic fracture mechanics analysis can be used to assess the cracks revealed from inspections. For bridges with cracks operating at temperatures above the transition temperature, elastic-plastic fracture analysis must be conducted. Fatigue growth rates must also be considered when developing the inspection and maintenance scheduling for distressed bridges. This section presents a procedure for fracture analysis of FCMs.

(1) For brittle fracture analysis, the stress intensity factor ( $K_I$ ) shall always be less than the critical stress intensity factor ( $K_{Ic}$ ). The critical crack size ( $a_{cr}$ ) is related to material fracture toughness ( $K_{Ic}$ ) for a given applied load and loading rate at the minimum service temperature as follows:

$$a_{cr} = [K_{Ic} / (F.S. \beta \sigma)]^2 \quad (4-1)$$

where

$a_{cr}$  = critical crack size in inches

$K_{Ic}$  = fracture toughness of the bridge material in ksi times square root of inches

$F.S.$  = appropriate factor of safety (e.g., 2)

$\beta$  = constant which is a function of crack and joint geometry, loading type, and welding-induced residual stress

$\sigma$  = applied nominal stress in ksi

(2) For ductile fracture analysis, CTOD is usually used to calculate crack criticality. An effective crack parameter, equivalent to the through thickness dimension of the joint which would yield the same stress intensity factor as the actual crack under the same load, is used to compare with the critical CTOD values of the bridge material. This effective crack parameter shall not be greater than the critical CTOD.

b. The procedure for fracture assessment of cracks is discussed by Tsai and Shim (1992) and is summarized below:

(1) Determine the actual shape, location, and size of the discontinuity by NDT inspection.

(2) Determine the effective crack dimensions to be used for analysis. Cracks are classified as through thickness (may be detected from both surfaces), embedded (not visible from either surface), or surface (may be observed on one surface). Through thickness cracks may be detected and defined by visual, dye penetrant, magnetic particle, or ultrasonic methods. Embedded cracks may be detected by ultrasonic and possibly radiographic methods. To determine the effective dimensions of a single crack or multiple cracks:

(a) Resolve the crack(s) into a plane normal to the principle stresses.

(b) Determine the effective dimensions for various isolated cracks. Check interaction with neighboring cracks to obtain the idealized crack dimensions.

(c) For surface or embedded cracks (idealized or actual), check their interaction with surfaces by recategorization.

(d) Determine final idealized effective dimensions for fracture analysis.

(3) Determine material properties including yield stress, Young's Modulus and  $K_{Ic}$  or CTOD.  $K_{Ic}$  may be estimated from Charpy V-Notch test (CVN) by Barsom's two-stage transition method (Barsom and Rolfe 1987) if direct  $K_{Ic}$  test data is not available.

(4) Idealize the total stresses by dividing them into primary stress,  $\sigma_p$ , and secondary stress,  $\sigma_s$ . The primary stress consists of membrane stresses,  $\sigma_m$ , and bending stress,  $\sigma_b$ , which include the effect of stress concentration imposed by geometry of the detail under consideration. Examples of the secondary stress include stress increase at re-entry angles in the joint, thermal, and residual stress. For cracks in welds, the residual tensile stress should be taken as yield stress. An estimate of the residual stress should be appropriate for post heat-treated weldments.

(5) Perform fracture assessment to determine the critical crack size. If applied stress is greater than the yield stress, CTOD must be employed. If applied

stress is less than the yield stress and the plane strain factor  $\beta_{Ic} < 0.4$  (Irwin's plane strain condition for brittle fracture), analysis must be based on  $K_{Ic}$ . When applied stress is less than the yield stress and  $\beta_{Ic} > 0.4$ ,  $K_c$  should be used instead of  $K_{Ic}$ .

(6) If the crack is subcritical, determine the remaining life using a fatigue analysis procedure. The upper limit for the brittle fracture behavior (plane strain behavior) is:

$$K_{Ic}/\sigma_{ys} = (t/2.5)^{0.5} \quad (4-2)$$

c. When this upper limit is exceeded, extensive plastic deformation occurs at the crack tip (crack tip blunting), and a nonlinear elastic plastic analysis must be used to assess the crack. CTOD is appropriate for this type of fracture analysis. The CTOD analysis procedure can be summarized as follows:

(1) Determine the effective crack parameter ( $\bar{a}$ ).

(a) For through thickness crack ( $= t/2$ ) where  $t$  is the crack size.

(b) For surface crack,  $\bar{a}$  is determined from Figure 4-1.

(c) For embedded crack,  $\bar{a}$  is determined from Figure 4-2.

(2) Determine allowable crack parameter  $a_m$ , which can be calculated by

$$\bar{a} \bar{a}_m = c \left( \frac{\delta_{crit}}{\epsilon_y} \right) \quad (4-3)$$

where

$\delta_{crit}$  = critical CTOD

$\epsilon_y$  = material yield strain

The constant  $c$  is determined from Figure 4-3. In determining  $c$ , if the sum of the primary and secondary stresses, excluding residual stress, is less than  $2\sigma_{ys}$ , the stress ratio  $(\sigma_p + \sigma_s)/\sigma_{ys}$  is used as the abscissa in Figure 4-3. If this sum exceeds  $2\sigma_{ys}$ , an elastic plastic stress analysis should be carried out to determine the maximum equivalent plastic strain which would occur in the region containing the crack if the crack was not present. The value of  $c$  may then be determined using the strain ratio,  $\epsilon/\epsilon_y$ , as the abscissa in Figure 4-3.

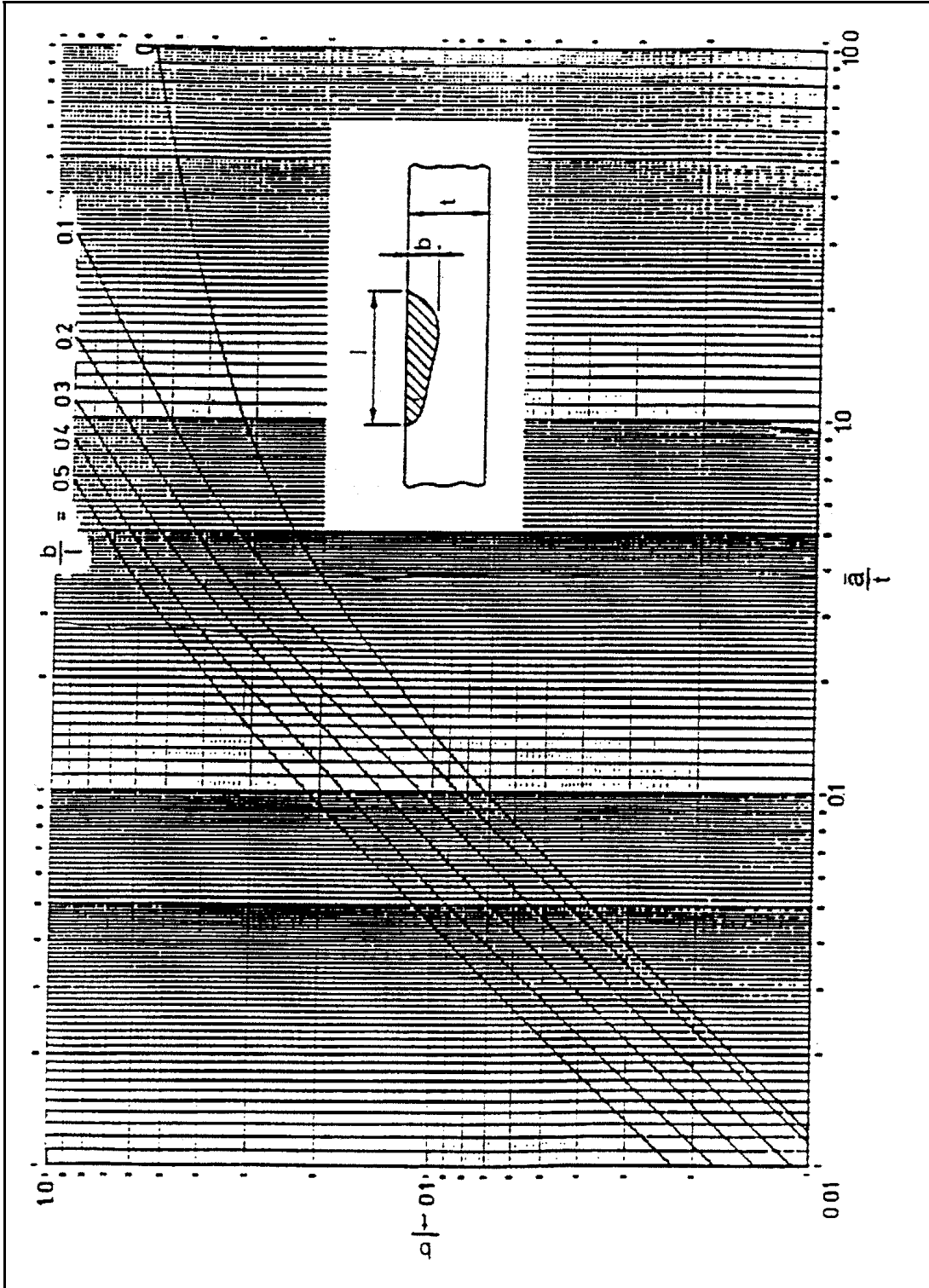


Figure 4-1. Relation between dimensions of a discontinuity and the parameter  $a$  for surface discontinuities

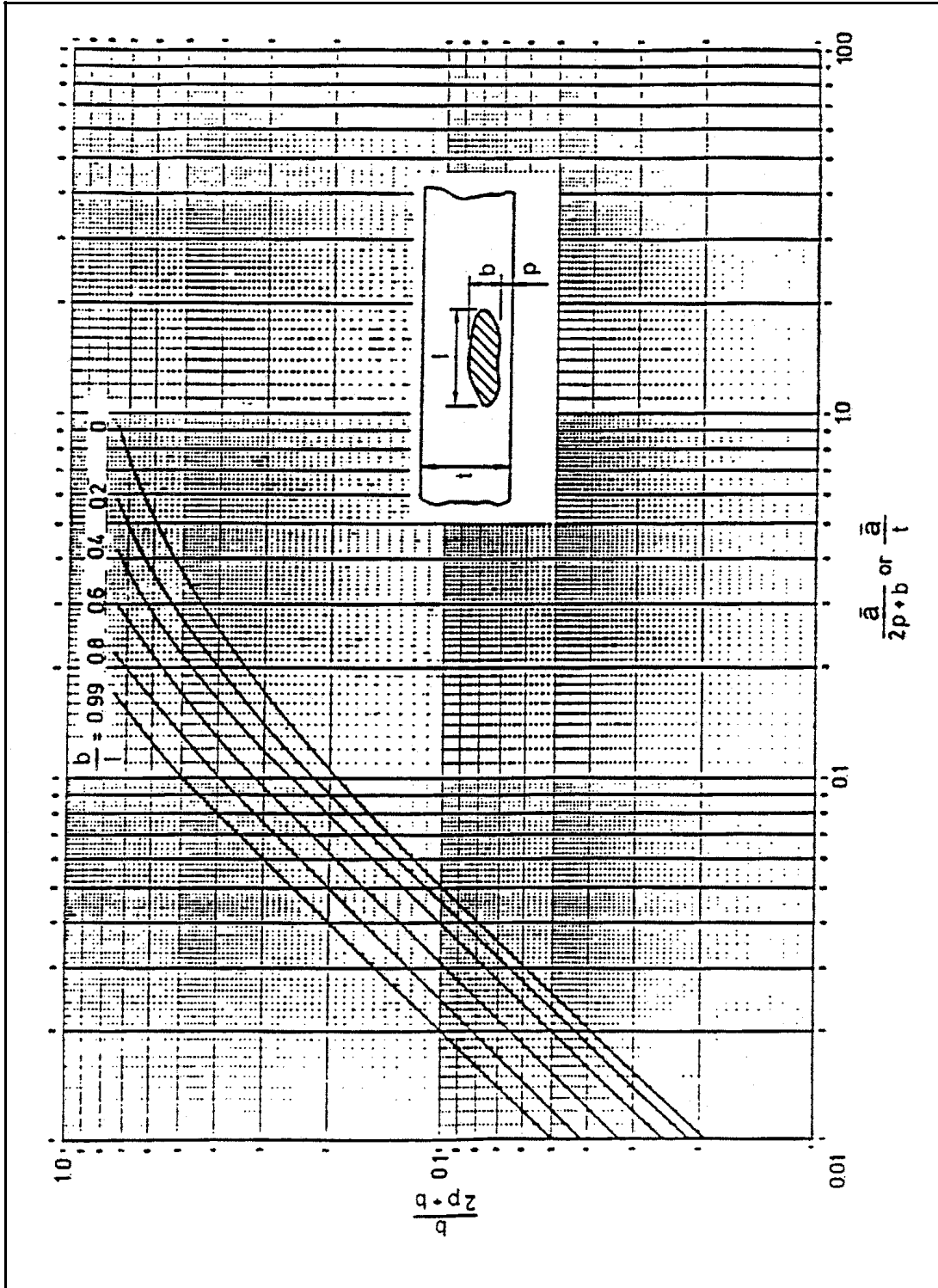


Figure 4-2. Relation between dimensions of a discontinuity and the parameter for embedded discontinuities

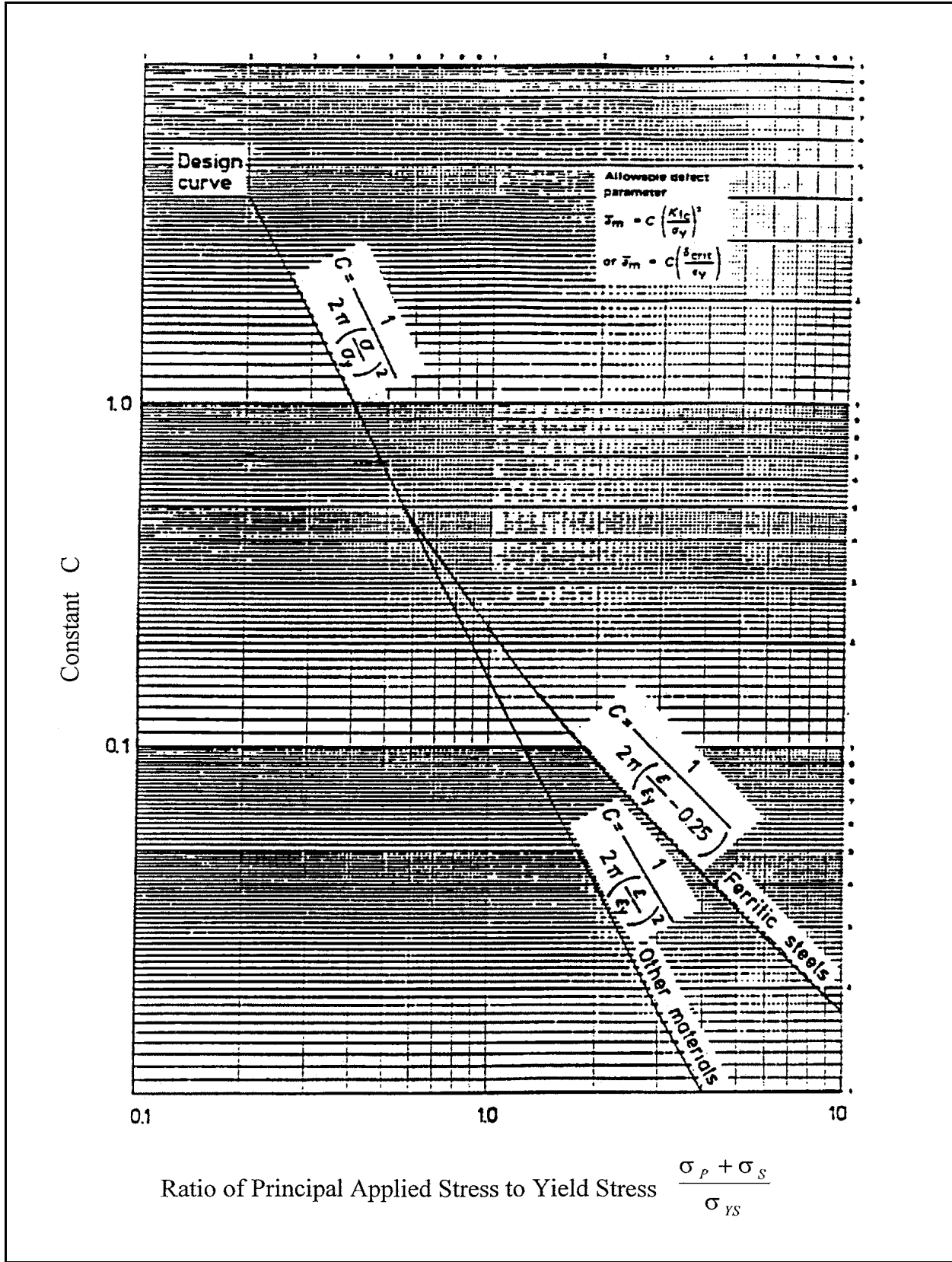


Figure 4-3. Values of constant c for different loading conditions

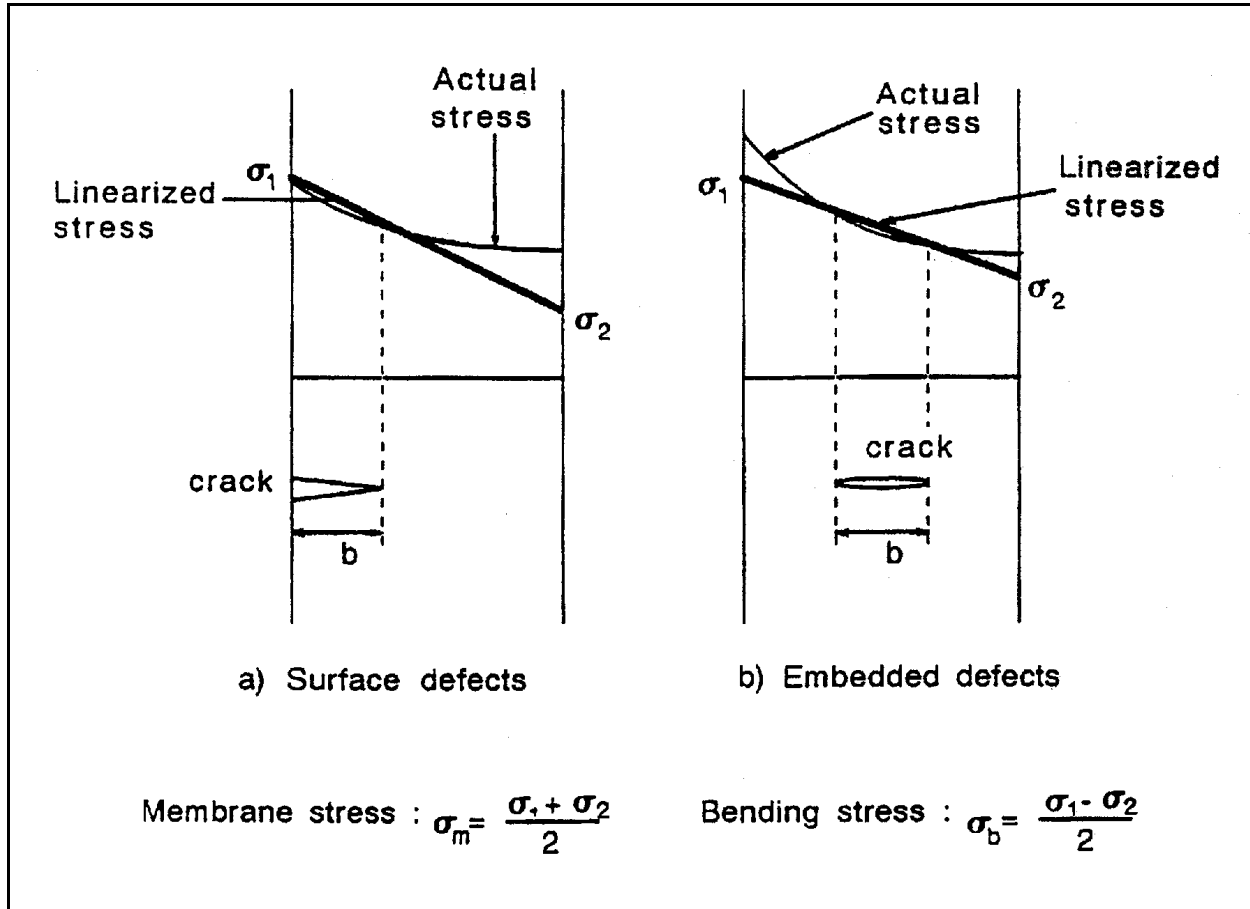


Figure 4-4. Linearization of stresses

(3) If the effective crack parameter,  $a$ , is smaller than the allowable crack parameter,  $\bar{a}_m$ , then the crack is considered stable under static loading. Using the procedure described in the second step above results in a safety factor of approximately 2.5 in determining  $\bar{a}_m$ . Therefore, the calculated critical crack size would be equal to  $2.5 \bar{a}_m$ .

#### 4-4. Fatigue Analysis Procedure

*a.* Dependent on the nature and fabrication of the joint detail, the joint fatigue characteristics are represented by the S-N curve of the appropriate category. While S-N curves are referenced to constant amplitude stress cycles, the stress cycles experienced by actual bridge structural details vary insignificantly in normal bridge operations. An equivalent constant stress range would cause the same damage and fatigue life as the actual stress range spectrum experienced in the field.

*b.* To evaluate the fatigue safety of an existing bridge structure, the maximum stress range should first be compared with the fatigue limit for the detail in question. Fatigue limit is defined as the constant amplitude stress range with which the detail can endure an unlimited number of cycles without developing fatigue cracks. If the maximum stress range is greater than the fatigue limit, fatigue cracking is expected after a number of stress cycles. The total fatigue life of the detail may be tens of millions of stress cycles, but not unlimited. Further application of loading after crack initiation would cause the crack to extend. Only after significant crack growth is the situation likely to become critical to the extent that the crack would become unstable and failure would occur. In general, fatigue cracks usually exist in structural members adjacent to weld toes.

c. The design S-N curves for various steel joint details are specified in the AWS D1.1 Structural Welding Code (American Welding Society 1992). Figure 4-5 shows a summary of fatigue categorization for various details of nonredundant structures used by the AWS welding code. To ensure conservative fatigue assessments, the code uses a mean minus 2 standard deviations (i.e., 97.7 percent survival probability) as the lower bound S-N curves for design purpose. The design S-N curves can be expressed as

$$\log N = \log A + m \log S \quad (4-4)$$

or

$$N = A S^m \quad (4-5)$$

where

$m$  = inverse negative slope of the S-N curve

$\log A$  = intercept of the  $\log N$  axis

$S$  = full stress range in ksi (i.e., applied maximum nominal stress minus applied minimum nominal stress)

$N$  = fatigue life in number of cycles

d. Redundant structures are those structures using redundant structural members. Failure of these members will not cause catastrophic structural failure. Therefore, the S-N design curves use a mean minus one standard deviation (i.e., 84.1 percent survival probability) as the lower bound for design purpose. Secondary bridge members, such as stiffeners, may apply the redundant structure S-N curves to assess the connection fatigue categories. However, fatigue cracks do not usually occur in these secondary stiffening members. For application simplicity, the nonredundant structure S-N curves are used for assessing the entire bridge structures.

e. Six fatigue categories are defined by the AWS D1.1-Structural Welding Code (American Welding Society 1992) for different joint details and stress types. Category F is for shear stress only and in most cases is used to categorize fillet welds. The AWS fatigue categories for redundant and nonredundant structures are shown in Figure 4-6 and the constants are summarized in Table 4-1.

f. The S-N curve design procedure is relatively simple to apply. However, this approach has some disadvantages. For example, S-N curves do not separate the stages of crack initiation and crack growth, the plasticity effects cannot be quantified, although they are included in the test data; and the local stress-strains at the weld toe are unknown where fatigue crack will inevitably initiate. Therefore, the S-N curve design procedure is used to plan a strategy for scheduled inspection and evaluation only. For those members found with cracks during the scheduled inspection, fracture mechanics and fatigue theory must be applied to estimate the remaining life of the distressed bridge members.

g. An accurate estimation of the number of stress cycles experienced to-date by a bridge structure requires knowledge of the operating history of the bridge. An average daily operation (ADO) curve may be established based on the bridge operating history. A possible source for historical operating information is an onsite operational control device, if one exists. The area under the ADO represents the total number of stress cycles experienced by the bridge within a specified period of time. Dependent on the operational characteristics of the bridge, each event may cause one or more stress cycles at a given detail. For example, vibration of the bridge may occur if it is harmonic with the vehicle crossing frequency. This vibration may induce more than one stress cycle at joint details. The natural frequency of the bridge should also be considered when estimating the number of stress cycles.

h. Occasionally, due to collision, (e.g., barge impact, falling ice or debris) during bridge operation, overload may occur in the bridge. This occasional overload may cause brittle fracture of cracked members. Therefore, brittle fracture should be considered when infrequent overload is possible. For frequent overload occurrence, the cumulative damage must be considered in the fatigue analysis. The root-mean-cube effective stress range may be used to estimate the total fatigue life using the constant-amplitude S-N design curves. To estimate the effect of known overloading history, Barsom's root-mean-square crack propagation model (Barsom and Rolfe 1987) may be used to estimate the remaining life of the cracked members.

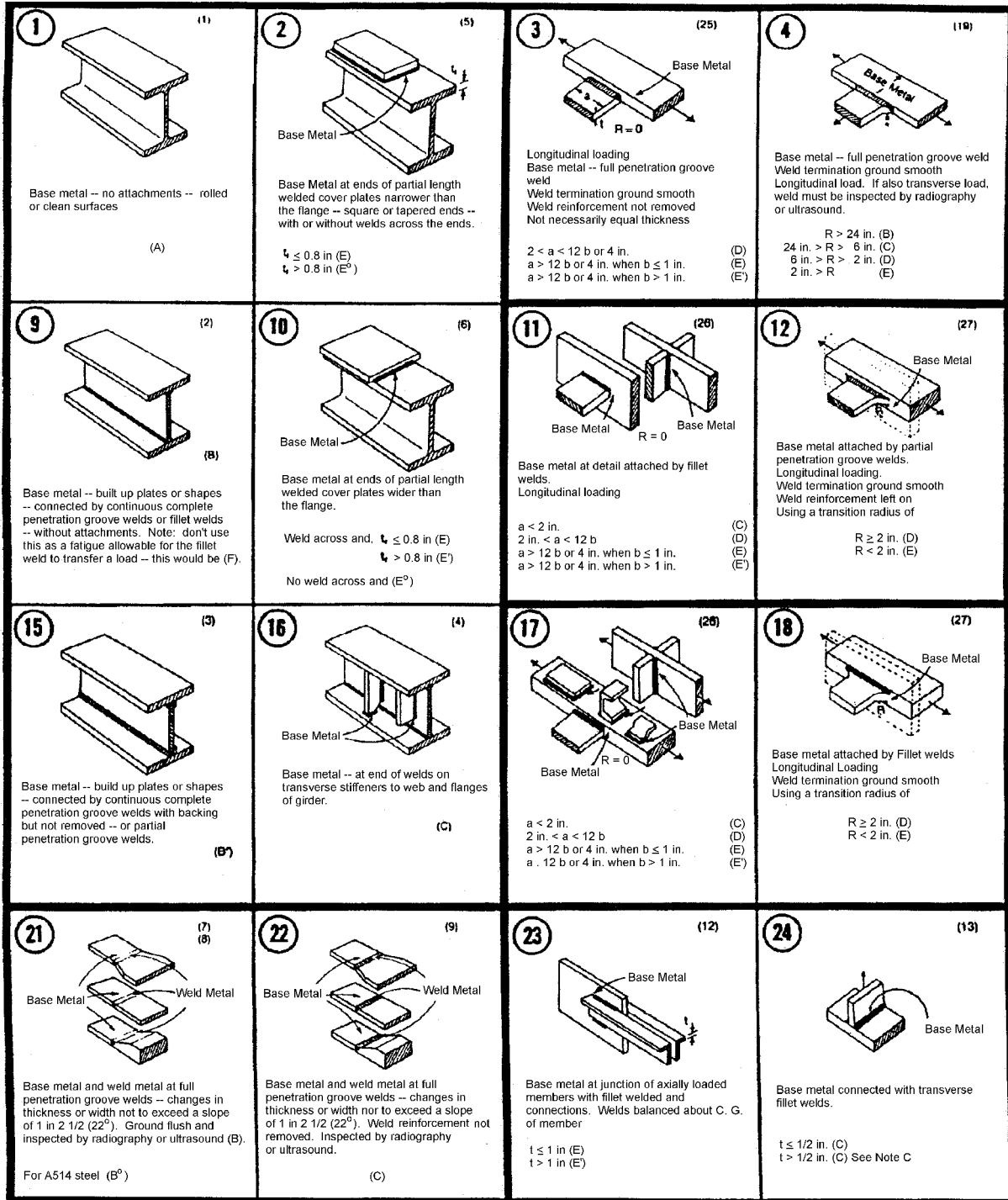
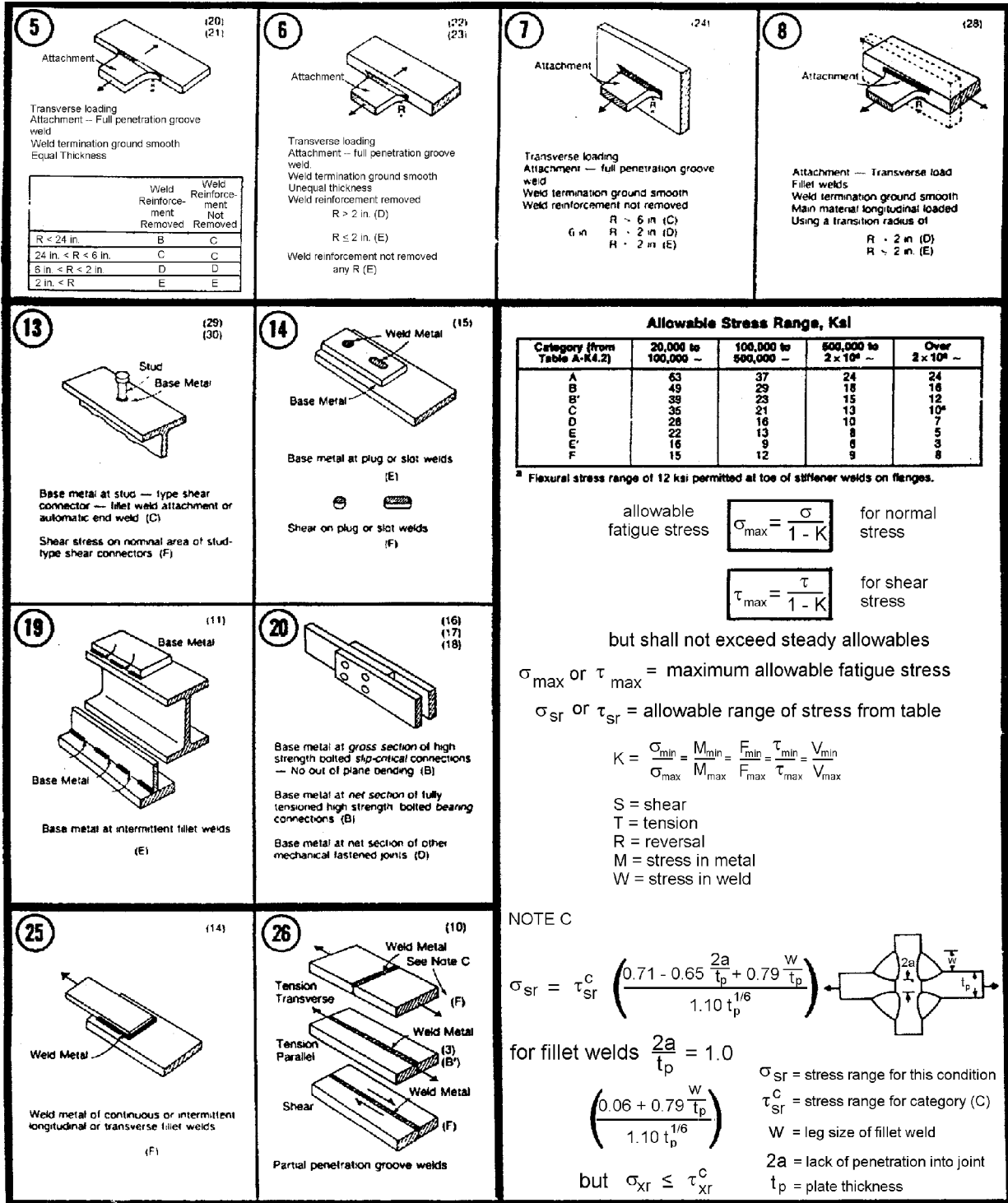


Figure 4-5. Summary of fatigue categorization for nonredundant structure details. Personal Communication from Omer W. Blodgett to Dr. Chon Tsai, Ohio State University, Columbus, OH (continued)



NOTE C

$$\sigma_{sr} = \tau_{sr}^c \left( \frac{0.71 - 0.65 \frac{2a}{t_p} + 0.79 \frac{W}{t_p}}{1.10 t_p^{1/6}} \right)$$

for fillet welds  $\frac{2a}{t_p} = 1.0$

$$\left( \frac{0.06 + 0.79 \frac{W}{t_p}}{1.10 t_p^{1/6}} \right)$$

but  $\sigma_{sr} \leq \tau_{sr}^c$

$\sigma_{sr}$  = stress range for this condition  
 $\tau_{sr}^c$  = stress range for category (C)  
W = leg size of fillet weld  
2a = lack of penetration into joint  
 $t_p$  = plate thickness

Figure 4-5. (Concluded)

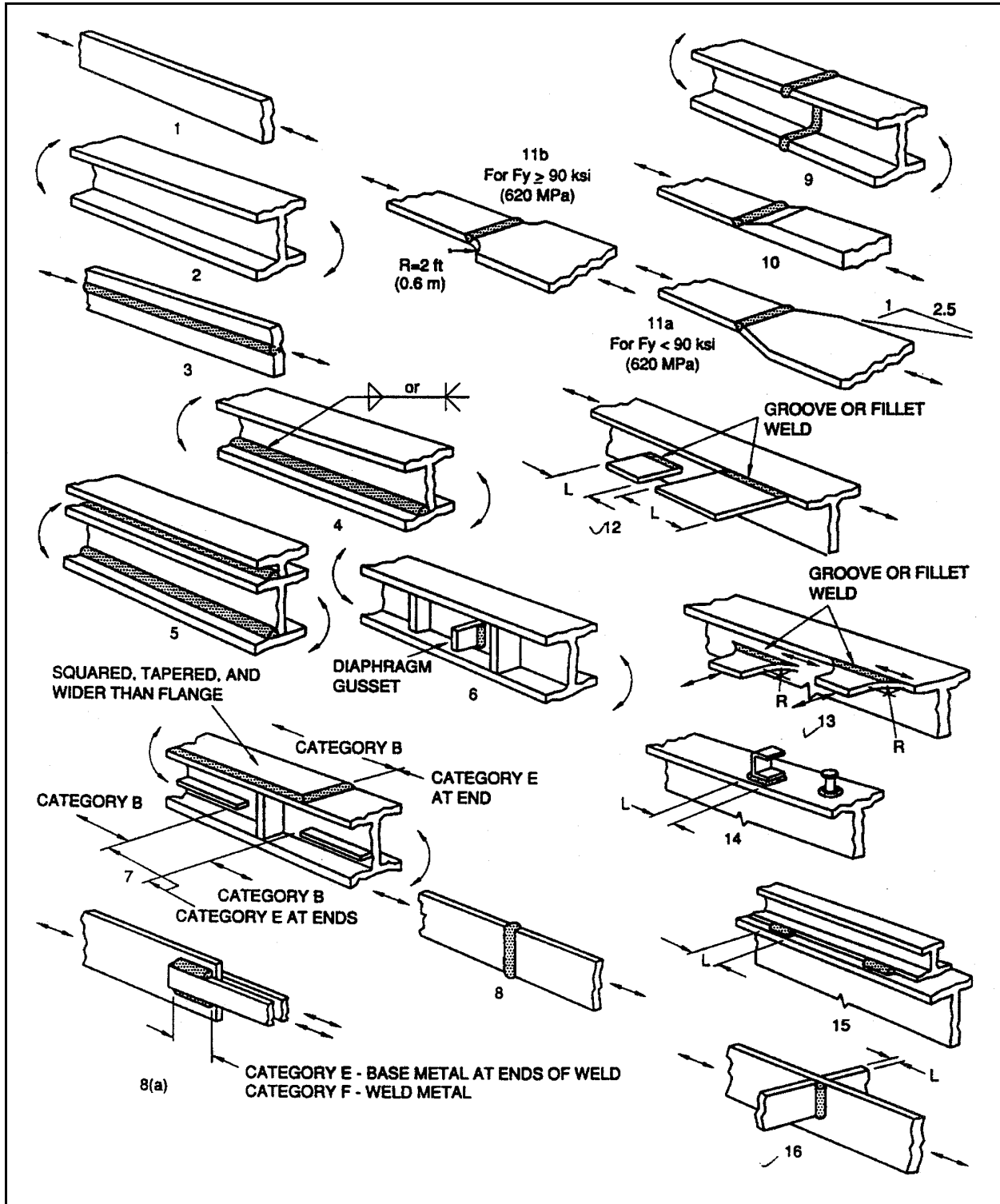


Figure 4-6. Fatigue categorization for nonredundant and redundant structure detail

**Table 4-1**  
**Fatigue Categories for Redundant and Nonredundant Structures**

<u>Category</u>	<u>Constant m</u>	<u>Constant A, cycles</u>	<u>Fatigue Limit, ksi</u>
<b><u>Nonredundant Structures</u></b>			
A	-4.76	$1.800 \times 10^{12}$	22.0
B	-3.73	$2.044 \times 10^{10}$	15.8
C (stiffeners)			
12.5 > S > 10.9	-18.18	$3.666 \times 10^{25}$	10.9
19.0 > S > 12.5	-5.93	$1.706 \times 10^{12}$	10.9
C (other attachments)	-5.93	$1.706 \times 10^{12}$	9.0
D	-3.75	$2.945 \times 10^9$	4.7
E	-3.85	$1.392 \times 10^9$	2.4
F 9.0 > S > 7.0	-9.88	$1.359 \times 10^{15}$	7.0
F S > 9	-6.74	$1.359 \times 10^{12}$	7.0
<b><u>Redundant Structures</u></b>			
A	-3.32	$8.070 \times 10^{10}$	21.7
B	-3.11	$1.466 \times 10^{10}$	15.5
C (stiffeners)	-3.29	$7.729 \times 10^9$	11.3
C (other attachments)	-3.29	$7.729 \times 10^9$	10.0
D	-2.98	$1.914 \times 10^9$	7.0
E	-2.99	$9.817 \times 10^8$	5.0
F	-5.68	$4.840 \times 10^{11}$	8.0

*i.* The cumulated fatigue damage degree (i.e., without crack found in the member) is estimated by comparing the cycles to date with the total fatigue life. The difference between these two values is the remaining fatigue life. The remaining fatigue life converted into a length of time is dependent upon the projected ADO curve. A scheduled inspection and evaluation plan for the bridge can be developed based on the projected remaining fatigue life.

*j.* A practical procedure for the estimation of fatigue life can be summarized as follows:

(1) Examine the structural detail in question and determine its fatigue category.

(2) Estimate the maximum full stress range, which must reflect the extreme stress values caused by overloads.

(3) If the maximum full stress range does not exceed the fatigue limit of the structural detail in question, fatigue cracking is unlikely to occur. The

fatigue life is taken as infinite. Additional assessment is unnecessary at this time.

(4) If the maximum full stress range exceeds the fatigue limit of the structural detail in question, the fatigue life is not infinite, and the risk of fatigue cracking must be assessed. The total fatigue life is determined using the appropriate S-N relationship.

(5) Use the ADO information to determine the stress cycles to date and the remaining fatigue life. Use projected ADO information to convert the remaining life cycles to number of years. If the remaining fatigue life is judged to be inadequate, retrofitting or strengthening measures should be considered to extend the bridge life.

#### **4-5. Prediction of Crack Growth**

*a.* Fatigue is a process causing cumulative damage from repeated loading. Fatigue damage occurs at stress concentrated regions where the localized stress exceeds the material yield stress. After a certain

number of load cycles, the accumulated damage results in crack initiation, as well as propagation. Fatigue life is the sum of the total number of cycles required to initiate a crack and propagate the crack to failure.

$$N_T = N_i + N_p \quad (4-6)$$

where

$N_T$  = total number of life cycles

$N_i$  = initiation life

$N_p$  = propagation life

Fatigue assessment is performed to determine the remaining life of a bridge.

*b.* A crack under repeated loading could be a nonpropagating crack. Tensile plastic strains developed at the crack tip during the initial tensile loading can result in compressive residual stresses upon unloading. If subsequent tensile loading is not sufficient to reopen this closed crack tip, the crack will not grow. Therefore, for a crack to propagate, the stress intensity factor must exceed a threshold value. The threshold values given below are applicable to martensitic, bainitic, ferrite-pearlite, and austenitic steels, which are the primary bridge steels (Barsom and Rolfe 1987).

$$\Delta K_{th} = 6.4(1 - 0.85R) \text{ ksi sqt(in) for } R > 0.1 \quad (4-7)$$

$$\Delta K_{th} = 5.5 \text{ ksi sqt(in) for } R < 0.1 \quad (4-8)$$

where

$R$  = the fatigue ratio which can be defined as the ratio of minimum stress to the maximum stress

$\Delta K_I$  = stress intensity factor range which is determined using the full applied stress range (i.e., the maximum stress minus the minimum stress) for welded structures

*c.* The crack will propagate according to Paris's power law of propagation if the stress intensity factor range is greater than the threshold value (Barsom and Rolfe 1987). Ferritic-pearlitic steels such as ASTM A36 and A572 Grade 50 steels are commonly used in

bridge construction. For welded steel bridges fabricated with this type of material, the following crack growth rate equation has been developed:

$$da/dN = 3.6 \times 10^{-10} (\Delta K_I)^3 \quad (4-9)$$

*d.* Crack growth rate accelerates as the subcritical crack approaches its critical dimension. Catastrophic fracture of the distressed bridge structural member will occur when the stress intensity factor at the maximum load reaches the critical fracture toughness value (i.e.,  $K_I = K_{Ic}$ ).

#### **4-6. Fracture and Fatigue Assessment Procedures**

*a.* The following fracture and fatigue procedures have been used for assessing a bridge's fitness for service (Barsom and Rolfe 1987).

(1) On the basis of the inspection data, determine the maximum initial crack size  $a_o$  present in the distressed connections and calculate the associated  $K_I$ .

(2) Knowing  $K_{Ic}$  for the material and the nominal maximum design stress, calculate the critical crack size ( $a_{cr}$ ) that would cause failure by brittle fracture.

(3) Determine fatigue crack growth rate using Paris's power law.

(4) Determine  $K_I$  using the appropriate equation, the estimated initial crack size  $a_o$ , and the range of live load stress.

(5) Integrate the crack growth rate equation between the limits of  $a_o$  (at the initial  $K_I$ ) and  $a_{cr}$  (at  $K_{Ic}$ ) to obtain the life of the structure prior to failure. To identify inspection intervals, integration may be applied with the upper limit being the tolerable size ( $a_t$ ). A safety factor of 2 may be appropriate for some applications. Another consideration to specifying a tolerable crack size is the crack growth rate ( $da/dN$ ). The tolerable crack size ( $a_t$ ) should be chosen such that the crack growth rate ( $da/dN$ ) is relatively small and a reasonable length of time remains before the critical size is reached.

*b.* Large embedded cracks or surface cracks may be recategorized into an equivalent surface crack or a through-thickness crack, respectively. The crack recategorization procedure is as follows:

(1) For embedded cracks, assume that the crack grows until it reaches a circular shape. Subsequently, it grows radially and eventually protrudes a surface at which time it is treated as a surface crack.

(2) For surface cracks, the initial propagation will result in a semi-circular shape. Further propagation will result in the crack reaching the other surface, at which time it is treated as a through thickness crack.

#### 4-7. Development of Inspection Schedule

Inspection schedules can be developed from number of cycles versus crack size curves. Figure 4-7 shows a schematic curve of the number of cycles versus crack size, which can be obtained from integrating the crack growth rate equation (West 1982). The critical crack size is determined by equating the maximum  $K_I$  to  $K_{Ic}$ . Repair will be needed before the crack grows to the critical dimension ( $a_{cr}$ ). For some applications, repair might be made when the crack reaches one half the critical crack length (i.e., factor of safety 2). Inspection intervals may be determined by dividing the remaining life cycles into several intervals.

#### 4-8. Fitness-for-Service Assessment Procedure

A bridge is fit for service when it performs the intended structural functions satisfactorily in service during its lifetime without reaching any serious limit state. Fitness-for-service is the concept of developing a maintenance schedule to ensure structural reliability for the lifetime of the structure. Some essential constituents to be considered when determining a structure's fitness-for-service include design, materials, welding, fatigue, codes and standards, reliability analysis, fracture control plans, failure modes, and the effectiveness of the quality assurance program. The fitness-for-service assessment procedure presented in this section addresses the evaluation of distressed existing bridges. The procedure consists of the following five steps:

- *Description of general concerns.* The general concerns include structural performance of the distressed bridge, consequences of failure, political and economic impact, costs for further

inspection and repair, interruption of bridge operation due to further inspection or repair, and operation scheduling.

- *History review of the bridge and preliminary analysis.* This would include reviewing the design, drawings, performance functions, loading history, environmental conditions, properties of structural materials, welding procedures used, fracture control plan, and quality control documentation. Fatigue categorization of various joint details may also be necessary to select the appropriate S-N curve for life assessment, along with information pertaining to the location of FCMs.

- *Fracture and fatigue analysis.* After the bridge inspection has been performed, it may be necessary to perform fracture and fatigue analysis to determine if discontinuities are defects. The appropriate fracture criterion must be selected; idealization of the total stresses must be considered, and it may be necessary to recategorize the discontinuities identified in the field inspection. It may become necessary to calculate stress intensity factors and perform material testing to obtain information on the mechanical and chemical properties of the bridge members. For fatigue life estimation it may be necessary to use S-N curves and the Paris crack propagation law.

- *Fitness-for-service assessment.* With the analysis results and information obtained from the preceding steps, the life expectancy of the distressed bridge can be assessed based on the service requirements, as well as other considerations, such as, failure consequences and economic and scheduling impact due to repair or replacement of the distressed members. A fracture control plan can be developed at this time if one does not already exist.

- *Repair and damage control.* If the discontinuities are determined to be defects, a repair procedure must be developed to restore the distressed bridge to a level fit-for-service. A maintenance schedule must be developed based on the fracture and fatigue analysis to restore the bridge. If the discontinuities are determined to be noncritical at this time, then an inspection and evaluation schedule must be developed considering the estimated remaining bridge life and the calculated crack growth rate.

31 Aug 98

Initial crack length (in.)= 0.13  
Critical crack length (in.)= 1.07  
Life (cycles)= 0.23E+06  
Max. stress (ksi)= 17.9    Min. stress (ksi)= 0.0  
Stress ratio= 0.00  
Failure mode = instantaneous failure

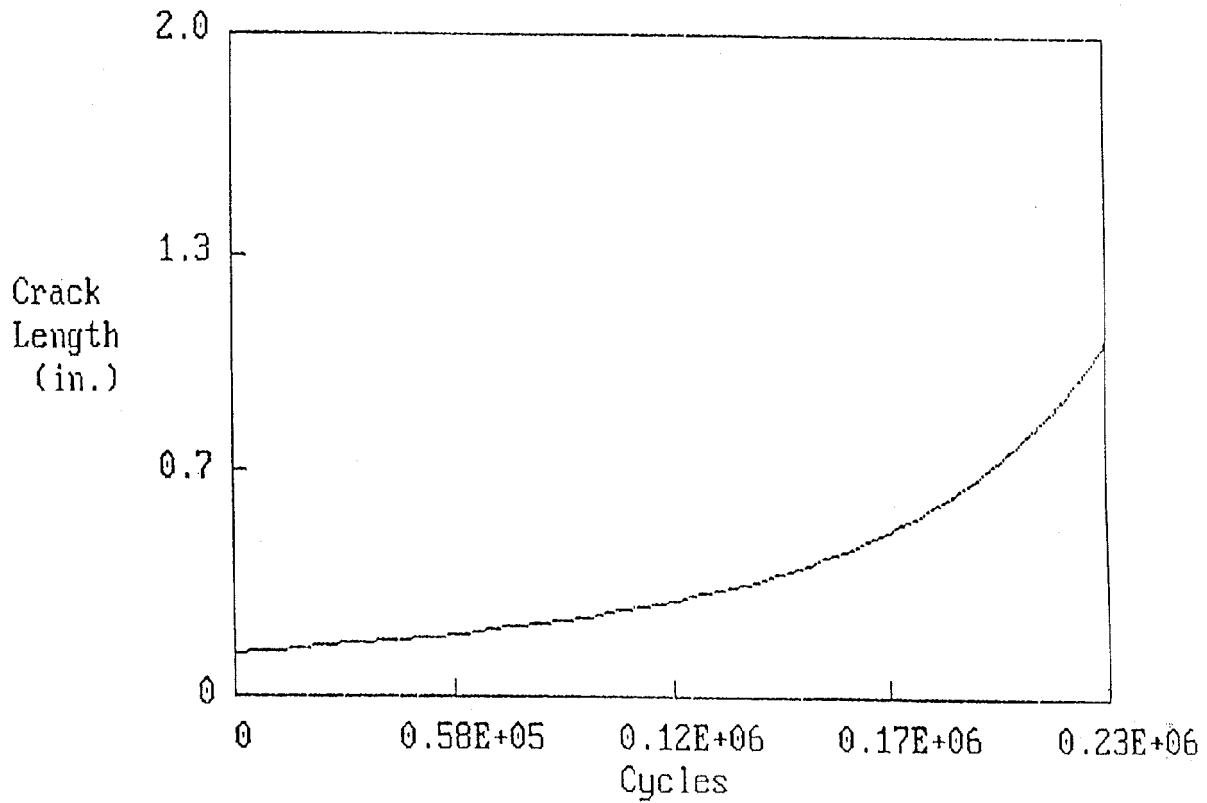


Figure 4-7. Relation between number of cycles and crack size

## **Chapter 5**

### **Conclusion**

This report provides information on how to identify fracture critical members in steel bridges. In addition, this report also provides guidance for

effective inspection and evaluation of the fracture critical members. The engineering critical assessment procedure presented in this report can be applied to assess the overall condition of a bridge and its fitness-for-service. Appropriate application of these procedures can assure public safety of in-service bridges.

## Appendix A References

### A-1. Required Publications

#### ER 1110-2-111

Periodic Safety Inspection and Continuing Evaluation of USACE Bridges

#### AASHTO 1983

AASHTO. 1983. "Manual for Maintenance Inspection of Bridges," Washington, DC.

#### AASHTO 1994

AASHTO. 1994. "Manual for Condition Evaluation of Bridges," Washington, DC.

#### AASHTO 1996

AASHTO. 1996. "Standard Specifications for Highway Bridges," Washington, DC.

#### American Welding Society 1980

American Welding Society. 1980. "Welding Inspection." Miami, FL.

#### American Welding Society 1985

American Welding Society. 1985. "ANSI/AWS B1.10 Guide for the Nondestructive Inspection of Welds." Miami, FL.

#### American Welding Society 1992

American Welding Society. 1992. "AWS D1.1 Structural Welding Code-Steel." Miami, FL.

#### ANSYS 1992

ANSYS. 1992. "ANSYS User's Manual," Swanson Analysis Systems, Houston, PA.

#### Asawa et al. 1982

Asawa, C. K., et al. 1982. "High-sensitivity fiber-optic strain sensors for measuring structural distortion," *Electronics Letters* 18(9), 362-363.

#### Azmi 1990

Azmi, M. 1990. "Acoustic emission detection and monitoring of highway bridge composites," 50(7), 3050-B.

#### Bagdasarian 1994

Bagdasarian, D. 1994. "Assessing Structural Integrity through Vibration Monitoring," *Materials Evaluation* 52(2), 147-149.

#### Barsom and Rolfe 1987

Barsom, J. M., and Rolfe, S. T. 1987. *Fracture and Fatigue Control in Structures: Applications of Fracture Mechanics*, 2nd ed., Prentice-Hall, New Jersey.

#### Bassim 1987

Bassim, N. M. 1987. "Macroscopic origins of acoustic emission," *Nondestructive Testing Handbook*, R. K. Miller and P. McIntire, ed., 2nd ed., Vol. 5, 46-61.

#### Beliveau 1987

Beliveau, J. G. 1987. "System identification of civil engineering structures," *Canadian Journal of Civil Engineering* 14, 7-18.

#### Beliveau and Huston 1988

Beliveau, J. G., and Huston, D. 1988. "Modal testing of cable-stayed pedestrian bridge," *Proceedings of the International Workshop on NDE for Performance of Civil Structures*, 193-202.

#### Berger 1992

Berger, H. 1992. "Nondestructive characterization of materials: The challenge of the 1990s," *Materials Evaluation* 50(2), 299-305.

#### Bhole et al. 1993

Bhole, V. M., et al. 1993. "Eddy current monitoring of spacers in coolant channel assemblies of nuclear reactor," *British Journal of NDT* 35, 133-139.

#### Billing 1984

Billing, J. R. 1984. "Dynamic loading and testing of bridges in Ontario," *Canadian Journal of Civil Engineering* 11, 833-843.

#### Bray and McBride 1992

Bray, D. E., and McBride D. 1992. *Nondestructive Testing Techniques*. John Wiley & Sons, New York.

**Bray and Stanley 1989**

Bray, D. E., and Stanley, R. K. 1989. *Non-destructive Evaluation*, McGraw-Hill, New York.

**Brennan 1988**

Brennan, B. W. 1988. "Dynamic polarimetric strain gauge characterization study," *Proceedings of SPIE--The International Society for Optical Engineering*, 77-89.

**Bull et al. 1995**

Bull, C. E., et al. 1995. "On-line monitoring using ultrasonics," *British Journal of NDT*, 35(2), 57-64.

**Civil Engineering 1987**

*Civil Engineering*. 1987 (Oct.). American Society of Civil Engineers, New York.

**Cruby and Colbrook 1992**

Cruby, C. B., and Colbrook, R. 1992. "Novel applications of NDT to the monitoring of manufacturing processes," *British Journal of NDT* 34(3), 109-115.

**Fang and Berkovits 1994**

Fang, D., and Berkovits, A. 1994. "Evaluation of fatigue damage accumulation by acoustic emission," *Fatigue Fract. Engng. Mater. Struct.* 17(9), 1057-1067.

**FHWA 1991**

FHWA. 1991. "Bridge Inspector's Training Manual 90," National Technical Information Service, Springfield, VA.

**Fisher et al. 1990**

Fisher, J. W., et al. 1990. "Fatigue crack detection and repair of steel bridge structures," *IABSE Workshop on Remaining Fatigue Life of Steel Structures*, Lausanne, Switzerland, 4-6.

**Fisher and Wood 1988**

Fisher, J., and Wood, J. 1988. "Experience with bridge and building structures and opportunities for NDE," *Proceedings of the International Workshop on NDE for Performance of Civil Structures*, 101-122.

**Flesch 1988**

Flesch, R. G., et al. 1988. "A Dynamic Method for the safety inspection of large prestressed bridges," *Proceedings of the International Workshop on NDE for Performance of Civil Structures*, 218-230.

**Glaser and Nelson 1992**

Glaser, S. D., and Nelson, P. P. 1992. "High-fidelity waveform detection of acoustic emissions from rock fracture," *Materials Evaluation* 50(3), 354-359.

**Gong et al. 1992**

Gong, Z., et al. 1992. "Acoustic emission monitoring of steel railroad bridges," *Materials Evaluation* 50(7), 883-887.

**Green 1988**

Green, R., Jr. 1988. "Current and emerging techniques for NDE of civil structures," *Proceedings of the International Workshop on NDE for Performance of Civil Structures*, 81-100.

**Harland et al. 1986**

Harland, J. W., et al. 1986. "Inspection of fracture critical bridge members," U.S. Department of Transportation, Federal Highway Administration, Report FHWA-IP-86-26, National Technical Information Service, Springfield, VA.

**Hartle et al. 1991**

Hartle, R. A., et al. 1991. "Bridge inspector's training manual 90," Federal Highway Administration, Report FHWA-PD-91-015, National Technical Information Service, Springfield, VA.

**Hearn and Cavallin 1997**

Hearn and Cavallin. 1997.

**Hearn and Testa 1993**

Hearn, G., and Testa, R. B. 1993. "Resonance monitoring of building assemblies for durability test," *Journal of Testing and Evaluation* 21(4), 285-295.

**Hopwood and Prine 1987**

Hopwood, T., and Prine, D. W. 1987. "Acoustic emission monitoring of in-service bridges," PB88-24423/GAR; PB89-113666/GAR.

**Hugemaier 1991**

Hugemaier, D. J. 1991. "Nondestructive testing developments in the aircraft industry," 49(12), 1470-1478.

**Hutton and Skorpik 1975**

Hutton, P. H., and Skorpik, J. R. 1975. "Acoustic emission methods for flaw detection in steel highway bridges," Phase I and II, Federal Highway Administration Report No. 78-98, Battelle Pacific Northwest, Richland, WA.

**International Institute of Welding 1990**

International Institute of Welding. 1990. "IIW Guidance on Assessment of the Fitness for Purpose of Welded Structures," IIW/IIS-SST-1157-90.

**International Society for Optical Engineering 1988**

International Society for Optical Engineering. 1988. *A Proceedings of SPIE--The International Society for Optical Engineering*, Boston, MA.

**Kao 1988**

Kao, C. K. 1988. *Optical Fiber*, Peter Peregrinus, Ltd.

**Katsuyama and Matsumura 1989**

Katsuyama, T., and Matsumura, H. 1989. *Infrared Optical Fibers*, IOP Publishing, Ltd.

**Kishi and Ohtsu 1988**

Kishi, T., and Ohtsu, M. 1988. "Nondestructive evaluation of civil structures in Japan," *Proceedings of the International Workshop on NDE for Performance of Civil Structures*, M.S. Agbabian and S.F. Masri, ed., 63-80.

**Krautkrämer and Krautkrämer 1977**

Krautkrämer, J., and Krautkrämer, H. 1977. *Ultrasonic Testing of Materials* (2nd ed.).

**Lapp et al. 1988**

Lapp, J. C., et al. 1988. "Segmented-core single-mode fiber optimized for bending performance," *Journal of Lightwave Technology* 6(10), 1462-1465.

**Lew 1988**

Lew, H. S. 1988. "Nondestructive testing," American Concrete Institute.

**Libby 1971**

Libby, H. L. 1971. *Introduction of Electromagnetic Nondestructive Test Methods*, John Wiley and Sons, New York.

**Lord 1980**

Lord, A. E. 1980. "Acoustic emission--An update in physical acoustics," Vol XV, W. P. Mason, ed., Vol 15.

**Maria et al. 1989**

Maria, L. D., et al. 1989. "Absolute fiber-optic interferometric strain sensor with insensitive leading fiber," *Springer Proceedings in Physics* 44, H. J. Arditty, ed., 47-52.

**Marvin and Ives 1984**

Marvin, D. C., and Ives, N. A. 1984. "Wide-range fiber-optic strain sensor," *Applied Optics* 23(23), 4212-4217.

**Measures 1988**

Measures, R. M., et al. 1988. "Structurally integrated fiber optic strain rosette," *Proceedings of SPIE--The International Society for Optical Engineering*, 32-42.

**Morton et al. 1974**

Morton, T. M., et al. 1974. "Effect of loading vibration on the acoustic emissions of fatigue-crack growth," *Experimental Mechanics* 14(5), 208-213.

**Muravin et al. 1993**

Muravin, G. B., et al. 1993. "Acoustic emission and fracture criteria," *Russian Journal of Nondestructive Testing* 29(8), 567-573.

**ETL 1110-2-551**  
**31 Aug 98**

**Nestleroth 1993**

Nestleroth, J. B. 1993. "The remote field eddy current technique for stress corrosion cracks detection and identification," *British Journal of NDT* 35, 241-246.

**Paris et al. 1963**

Paris, P. C., et al. 1963. "A critical analysis of crack propagation laws," *Transactions of the ASME* 85, Ser. D, 528-534.

**Pollock and Smith 1972**

Pollock, A. A., and Smith, B. 1975. "Stress-wave emission monitoring of a military bridge," *Nondestructive Testing* 30(12), 348-353.

**Ramsamooj 1994**

Ramsamooj, D. V. 1994. "Prediction of fatigue life of plain concrete beams from fracture tests," *Journal of Testing and Evaluation* 22(3), 183-194.

**Scalzi 1988**

Scalzi, J. B. 1988. "Welcoming Remarks to the International Workshop on Nondestructive Evaluation for Performance of Civil Structures."

**Sharma et al. 1981**

Sharma, A. B., et al. 1981. *Optical Fiber Systems and Their Components*, Springer-Verlag.

**Stares et al. 1990**

Stares, I. J., et al. 1990. "On-line weld pool monitoring and defect detection using ultrasonics," *NDT International* 23(4), 195-200.

**Tardy et al. 1989**

Tardy, A., et al. 1989. "High sensitivity transducer for fiber-optic pressure sensing applied to dynamic mechanical testing and vehicle detection on roads," *Springer Proceedings in Physics* 44, 215-221.

**Thavasimuthu et al. 1993**

Thavasimuthu, M., et al. 1993. "Crack closure and ultrasonic examination--A few practical observations," *British Journal of NDT* 35(3), 125-128.

**Tsai 1990**

Tsai, C. L. 1990. "Fitness-for-Service Design of Welded Structures," The Ohio State University WE 740 Lecture Notes.

**Tsai and Shim 1992**

Tsai, C. L., and Shim, Y. L. 1992. "Structural Inspection and Evaluation of Existing Lock Gates," Technical Report, U.S. Army Engineer Waterways Experiment Station, Vicksburg, MS.

**Udd 1988**

Udd, E. 1988. "Overview of fiber optic smart structures for aerospace applications," *Proceedings of SPIE--The International Society for Optical Engineering*, 2-5.

**USACE 1940**

USACE. 1940. Summit Bridge Design Drawing No. 26582.

**USACE 1956**

USACE. 1956. St. Georges Highway Bridge Design Drawing No. 5251.

**Vannoy and Azmi 1991**

Vannoy, D. W., Azmi, M. 1991. "Acoustic emission detection and monitoring of highway bridge components," Final Report PB91-236273/GAR.

**West 1982**

West, W. 1982. "Shock Vibration Ball," 52(4), 25-31.

**West 1986**

West, W. 1982. "Illustration of the use of modal assurance criterion to detect structural changes in an orbit test specimen," *Proceedings of the Fourth International Modal Analysis Conference* 1-6.

**Wilson 1983**

Wilson, F. 1983. *Building Materials Evaluation Handbook*. Van Nostrand Reinhold Company.

**Wolfenden et al. 1989**

Wolfenden, A., et al. 1989. "Dynamic Young's Modulus measurements in metallic materials: Results of an interlaboratory testing program," *Journal of Testing and Evaluation* 17(1), 2-13.

**Wooh and Daniel 1994**

Wooh, S. C., and Daniel, Z. M. 1994. "Three-dimensional ultrasonic imaging of defects and damage in composite materials," *Materials Evaluation* 52(10), 1199-1206.

**Yao 1982**

Yao, J. T. P. 1982. *Solid Dynamics Earthquake Engineering*, 1(3).

**Yao et al. 1982**

Yao, J. T. P., et al. 1982. "Damage assessment from dynamic response measurement," *Proceedings of the Ninth United States National Cong. Applied Mechanics*, 315-322.

**Yuyama et al. 1994**

Yuyama, S., et al. 1994. "Acoustic emission evaluation of structural integrity of repaired reinforced concrete beams," *Materials Evaluation* 52(1), 86-90.

**A-2. Related Publications**

**American Society of Civil Engineers Audio Conference Notes 1992**

American Society of Civil Engineers Audio Conference Notes. 1992. "Bridge Inspection of Fracture Critical Members."

**Hariri 1990**

Hariri, R. 1990. "Acoustic emission investigation and signal discriminations in steel highway bridge applications, dissertation abstracts international," 51(3), 1399.

**Prikhod'ko and Fedorishin 1993**

Prikhod'ko, V. N., and Fedorishin, V. V. 1993. "Ultrasonic inspection of intergranular corrosion of stainless steel weld joints," *Russian Journal of NDT* 29(11), 799-807.

**Yen et al. 1990**

Yen, B. T., Huang, T., Lai, L. Y., and Fisher, J. W. 1990. "Manual for Inspecting Bridges for Fatigue Damage Conditions," Department of Civil Engineering, Fritz Engineering Laboratory, Bethlehem, PA.

## Appendix B

### A Review of State-of-the-Art Techniques for Real-Time Damage Assessment of Bridges

#### B-1. Introduction

*a.* It was reported that, as of November 1991, 35 percent of approximately 590,000 bridges in the United States were considered structurally deficient or functionally obsolete (Bagdasarian 1994). Many bridges have become deficient due to increased age and larger than expected service loads. In addition, some highway and railroad bridges ranging from 50 to more than 100 years old are still performing their intended function in spite of excessive use (Scalzi 1988). AASHTO has developed a “Manual for Condition Evaluation of Bridges” (1994), which provides for uniformity in the procedures and policies for determining the physical condition, maintenance needs, and load capacity of highway bridges. Recent bridge collapse or near collapse has focused the need to develop extensive nondestructive evaluation (NDE) techniques for real-time structural damage assessment to guarantee the safety of our nationwide transportation system. Real-time NDE techniques can immediately provide information such as size, shape, location, and orientation of discontinuities as part of the structural damage assessment.

*b.* NDE techniques for material inspection have been well-known for many years (Krautkrämer and Krautkrämer 1977; Lord 1980; Lew 1988; Bray and McBride 1992). They include liquid penetrant, eddy current, radiography, magnetic particle, ultrasonic, acoustic emission, and dynamic property measurement methods. Among those, ultrasonic and acoustic emission technologies have become the most popular and frequently used to perform real-time inspection. The dynamic property measurement method has also been used to evaluate the integrity of structures.

*c.* Applications of dynamic property measurement techniques in civil engineering (e.g., buildings, bridges, and dams) are rather rare. Although

the acoustic emission technique was suggested in the 1970s to monitor a military bridge (Pollock and Smith 1972) and to detect discontinuities in steel highway bridges (Hutton and Skorpik 1975), it was only successful in a limited number of instances (Fisher and Wood 1988). The reason for this may be multi-fold since NDE is an interdisciplinary technology. It involves mechanical, electromagnetic, acoustic, and optical techniques to evaluate the integrity of a structure. When it is used for civil engineering applications, such as bridge damage assessment, the discontinuities to be detected may be large in dimension but complex in structure. Moreover, the inspections are subjected to environmental influence such as weather and noise. Accessibility is also more of a challenge when performing field NDE on in-service bridges as opposed to inspecting items mass produced in a factory. In addition, there is less of a tendency for bridge features to be standardized relative to mass produced factory items. Consequently, “standard” NDE procedures for bridges typically do not exist but must be uniquely developed for each application. Nevertheless, with the combined strength of both the NDE tools and the civil engineering professionals, progress is being achieved in damage assessment of bridges.

*d.* Appendix B provides a brief review of NDE fundamentals and discusses their application towards evaluating fracture critical members (FCMs) on bridge structures. The principles and general applications of each technique are emphasized along with newly reported bridge field testing applications. Detailed knowledge pertaining to the physical bases and instrument operation procedures for each technique can be found in Krautkrämer and Krautkrämer (1977) and Bray and McBride (1992).

#### B-2. Some New NDE Techniques in Real-Time Structural Damage Assessment

*a.* *Eddy current method.*

(1) Principle.

(a) The eddy current method is based on the fundamental work of Farady, Oersted, and

Maxwell (Libby 1971). An electrical current flowing in a wire generates an electromagnetic field about the wire. The electro-magnetic field becomes concentrated when the wire is wound in the form of a coil. Such coils are used for the eddy current testing of materials. When an energized coil is placed near the surface of metallic material, eddy currents are induced in the material. Coil current must be alternating (ac), since relative motion between the field and conductor is required to generate or induce electricity. Current induced in the metal flows in a direction opposite to the current in the coil. Material properties as well as discontinuities, such as cracks or voids, will affect the magnitude and phase of the induced current. Thus, with the aid of suitable instrumentation, eddy currents can assess the material conditions. Typical test coil arrangements are shown in Figure B-1.

(b) The eddy current inspection method has numerous favorable characteristics that make it the proper choice for many inspection tasks. Primary among these advantages is that mechanical contact is not required between the eddy current transducers and the test articles. Eddy current penetration depth and, consequently, inspection depth can be controlled by adjusting the frequency of energizing current. The method has high sensitivity to small discontinuities. Dimensional measurements and electrical conductivity measurements can also be made. Instrumentation for eddy current testing is relatively low cost for most applications. The equipment can be automated for high-speed testing with lightweight portable instruments.

(c) Eddy current techniques are limited in that only electrically conductive materials can be tested. There is limited material penetration with high-frequency energy, and discontinuity indications are largely qualitative. The many material, geometric, and electronic parameters affecting test results often complicate data interpretation. Thus, considerable care must be exercised in selecting eddy current techniques and in evaluating inspection results to avoid interpretation errors.

## (2) Applications.

(a) As early as the late 1930s and early 1940s, investigators began the application of eddy current techniques to materials evaluation problems. Commercial instruments became available during this time and were used extensively during World War II.

(b) With the rapid development of electronics and computer science, presently the eddy current technology can be utilized to assess selected material properties as well as locate discrete discontinuities in metallic structures such as aircraft (Hugemaier 1991), coolant channel assemblies of nuclear reactor (Bhole et al. 1993), large diameter pipeline steels (Nestleroth 1993), etc. A list of selected applications is given in Table B-1.

(c) The establishment of accept/reject criteria for discontinuities is a matter of specifying how many discontinuities are acceptable, what size and how close together they are, if they can be allowed in engineering components of each class, material thickness, type of material, type of weld, size of structure, and service condition. Acceptance criteria are highly item oriented.

## (3) Inspection of bridges.

(a) Although not commonly used in inspecting steel bridges, eddy current method was reported to have been used to inspect steel bridges in Japan (Kishi and Ohtsu 1988). The onsite eddy current system used for steel highway bridges has advantages such as, clear reproduction of results, high inspection speed, no coating removal required, and feasibility for noncontact applications. However, there are still some problems in using eddy current methods to inspect welded members in steel bridges. One problem is the presence of noise in the electric current during field testing. Electronic noise signals can hamper the inspector's ability to identify discontinuities. Another concern is the significant disturbance from the spatial distribution of welded

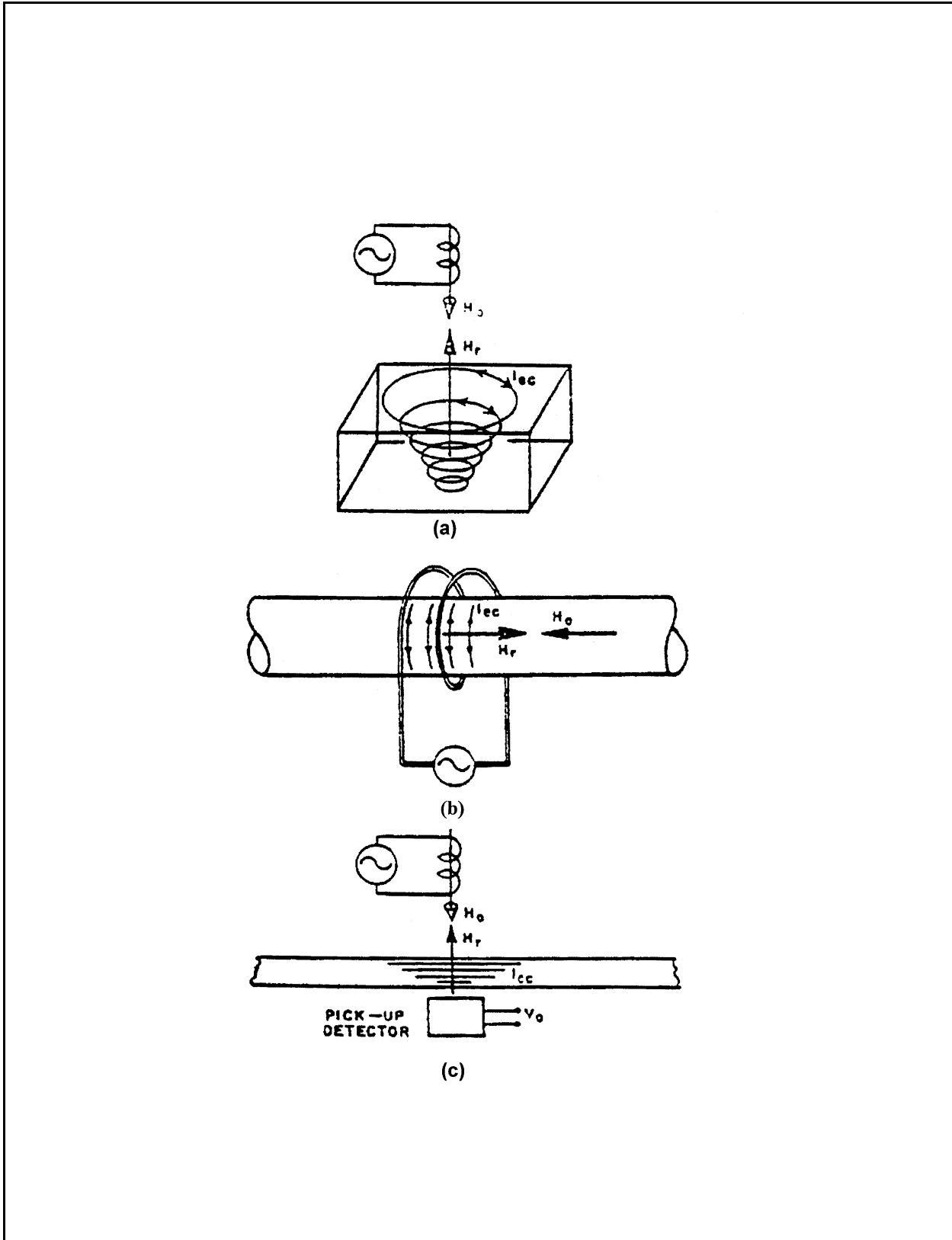


Figure B-1. Arrangements of eddy current test probes and test objects for (a) probe on one side of test object, (b) probe encircling test object, and (c) excitation and pick-up on opposite sides of test object

**Table B-1**  
**Typical Applications of Eddy Current Inspection**

Material Property Determinations

Heat treatment evaluation  
Hardness measurements  
Fire damage determinations  
Impurity content measurement

Discontinuity Detection

Sheet metal  
Foil  
Wire  
Bar  
Tube Testing  
Bolt inspection  
Weld inspection  
Ball bearings tests

reinforcement, which makes the separation between signal and noise also difficult to interpret. These problems are circumvented by self-compensating the permeability difference between weld metal and base metal and by minimizing noise signals due to reinforcement distribution.

(b) Eddy current signals from different types of discontinuities in steel girders are shown to be remarkably different, which may give useful information pertaining to structural damage assessment. Unfortunately, detailed information on measurements and interpretations of these signals have not been reported. Additional information on the eddy current method can be found in Bray and Stanley (1989) and AWS (1980).

*b. Vibration dynamic method.*

(1) Principle.

(a) Certain properties of structures can be evaluated using vibration dynamic techniques. It is well-known that a structure possesses certain natural vibration frequencies and mode shapes. If friction is taken into account, the vibrations that are already excited will decrease gradually. This is called a damping vibration. The dynamic vibration tests are carried out by applying a known forced vibration to the structure and observing its vibration response. The fundamental concept is to

compare to measured dynamic response with either the dynamic response predicted by an analytical model or the previously measured dynamic response.

(b) Theoretically, any discontinuities, cracks and other variations in structural properties will alter the vibration characteristics of the structures. Changes in vibration measurement may be used for structural damage assessment and monitoring bridge integrity. However, difficulties in modeling the restraint from supports as well as other modeling difficulties can preclude the comparison of modeled versus measured dynamic response to identify the subtle effects of cracks. In addition, environmental effects such as thermal expansion or debris collecting at expansion joints can also overshadow subtle changes in dynamic response due to the presence of cracks when comparing dynamic response to previous responses.

(c) Some fundamental modes of vibration for a very simple structure are illustrated in Figure B-2, which shows a fundamental flexural (a) and longitudinal (b) mode of vibration of a rectangular bar. For the flexural mode, the particle excursions in the material are vertical through the bar length; conversely, the particle excursions for the longitudinal mode are in the direction of the bar length. The natural vibration frequencies for these two modes can be written respectively as (for a square bar):

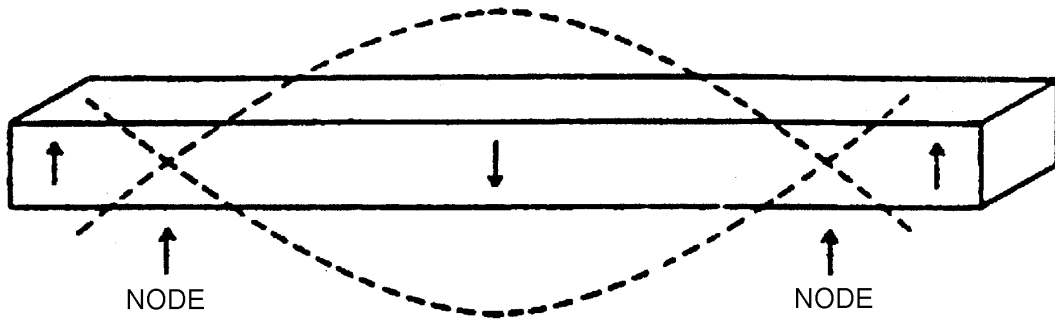
$$f_{flex} = \frac{20.2h}{l^2} \sqrt{\frac{E}{\rho}} \quad (B-1)$$

$$f_{long} = \frac{h}{2l} \sqrt{\frac{E}{\rho}} \quad (B-2)$$

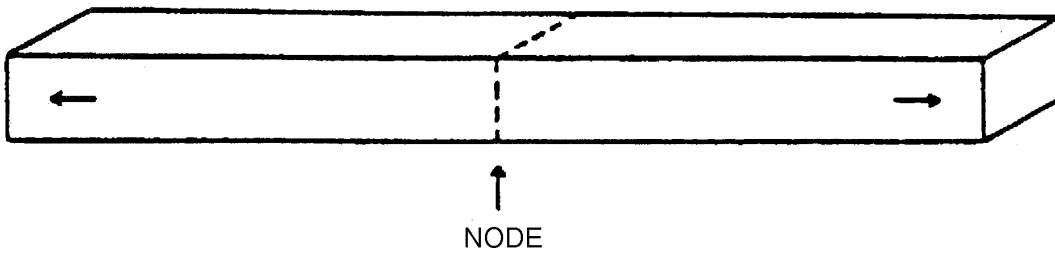
where

$f$  = natural vibration frequency (Hz)

$h$  = height or depth of the bar (in.)



a. Flexural mode



b. Longitudinal (extensional) mode

Figure B-2. Fundamental mode of vibration of a rectangular bar

$l$  = length

$\rho$  = density

If the natural vibration frequency is measured, the Young's Modulus of the bar can be obtained from Equation B-3, which suggests that Young's Modulus  $E$  is closely related to the natural vibration frequency. Young's Modulus is one of the important parameters for bar-like members such as beams in bridges. Young's Modulus for a square bare is calculated by

$$E = \frac{0.00245f^2l^4\rho}{h^2} \quad (\text{B-3})$$

(d) Real solids are never perfect; therefore, some of their mechanical energy is always converted into heat. This will lead to a vibration damping. Measurements of the vibration damping may provide reliable information for structural damage assessment.

(e) Mode shape is related to the structure properties. For the ideal solid bar mentioned above, the mode shape is very narrow with a high peak. But for more complicated structures, such as bridges, the mode shape depends on the mechanical properties and the geometric form of the structure.

(f) Hearn and Testa (1993) present a general equation of free vibration motion for an undamped elastic structure.

$$[K - \omega^2 * M] \{\phi\} = 0 \quad (\text{B-4})$$

where

$K$  = stiffness matrix

$M$  = mass matrix

$\omega$  = resonant frequency

$\phi$  = the vibration mode shape

A perturbation of the structure is considered in which a small change in stiffness  $[\Delta K]$  produces

small changes in eigenvalues  $\Delta(\omega^2)$  and in vibration mode shapes  $\{\Delta\phi\}$ , making the equation for the perturbed form

$$[(K + \Delta K) - (\omega^2 + \Delta(\omega^2))M] \{\phi + \Delta\phi\} = 0 \quad (\text{B-5})$$

Equation B-5 clearly shows the relation of the stiffness change with the changes of the natural frequency and mode shape.

## (2) Applications.

(a) A partial list of physical quantities that may be measured by these techniques is given in Table B-2. The experimental results of the dynamic Young's Modulus by the vibration technique can be found in (Wolfenden et al. 1989).

**Table B-2**  
**Physical Quantities Typically Measured by Resonance Vibration**

Length, width, thickness diameter
Modulus of elasticity
Shear Modulus
Poisson's Ratio
Density
Modulus of rupture
Discontinuities or other inhomogeneities

(b) Resonance of a structure is reached when the frequency of an applied vibration force produced by piezoelectric transducer or electromagnetic vibration matches the natural frequency of vibration of the structure. Damage which plastically deforms a member would also be expected to change the stiffness and the frequency of resonance. A loss of stiffness may be detectable as decrease in the observed resonant frequency of the member.

(c) Many types of discontinuities and defects have been reported to have been detected in structures using the vibration dynamic method. This capability is usually carried out by the vibration interrogation of an undamaged structure or assembly at sufficient frequency levels and modes to establish trend data. By comparing the vibration scan of an identical part with this known

reference, or by comparing the vibration scan for a given structure with time, one can detect whether there has been a change. The relative magnitude of change can be an indication of damage. Vibration dynamic techniques have been developed specifically to detect discontinuities and defects in various materials.

(d) A successful technique relevant to the vibration testing method was developed by West (1982 and 1986) for the space shuttle orbiter body flap test specimen. Several damage sites that were not detected by conventional NDE techniques were correctly identified by this technique. West's technique can locate damage in certain types of structures reasonably well, but it is unable to determine the extent of the damage.

(e) Two areas that have received considerable attention in recent years are civil engineering structures and offshore oil platforms (Yao 1982 and Yoa et al. 1982). The goal of the work was to define a method of assessing the structural integrity of buildings after their exposure to overload.

### (3) Inspection of bridges.

(a) Civil engineering structures such as bridges, buildings, and dams have many natural frequencies below 100 Hz (Billing 1984). A high-powered hammer has been used to excite the resonant vibrations of these structures. Partly based on this information, Beliveau and Huston used an impact hammer as an exciting source to test a full-scale pedestrian bridge (Beliveau 1987 and Beliveau and Hutson 1988).

(b) The bridge tested is located on a bicycle path over Route VT 127 North of Burlington, Vermont. It has a span of 54.86 m (180 ft) between abutments and a treated timber deck width of 3.40 m (11 ft 2 in.) between center lines of the two main 0.91-m (36-in.) girders and cable-stay system. The cables have a diameter of 34.93 mm (1-3/8 in.), and the bottom flanges of the girders are 0.56 m (1 in. by 10 in.) plate.

(c) The equipment brought to the bridge site operated solely on batteries and included four accelerometers, a 53.38 N (12-lb) impact hammer, and a seven-channel frequency modulated tape recorder. The bridge was instrumented on three trips: first, for impact testing along the bridge centerline; then, for ambient vibration on a windy day; and lastly, for impact testing along one of the two main girders.

(d) The impact signal and two vertical acceleration signals were stored during the inspection on three channels of the tape recorder for further analysis in the laboratory. For center line testing, the hammer and accelerometers were located at the center of nine cross stringers located 5.64 m (18.5 ft) apart. For the torsion test, the impact hammer and accelerometers were located on two main girders at the ends of the nine cross members joining the two main girders. A four-channel spectrum analyzer was used to perform the data analysis.

(e) An average of three or four impact tests were used to arrive at a frequency response function of a particular accelerometer subjected to an impact load at another or the same location. These were then combined in the polyreference technique to obtain a best fit of the sum of complex exponential to the inverse Fourier transform of these frequency response functions. The natural frequencies of the bridge for the vertical and torsional vibrations are calculated by a similar method given by Hearn and Testa (1993). The experimentally obtained resonance frequencies are consistent with the theoretical results. The study indicates that the vibration dynamic method can be used to assess bridges. However, no further structural damage assessments using this method have been reported by the same investigators.

(f) The dynamic method has also been used for safety inspection of prestressed bridges in Austria (Flesch et al. 1988). The basic concept is the same: damage of the structure will lead to deviations of the dynamic parameters from the

virgin state. These deviations can be used in a global manner to assess damage. In this report, emphasis was put on the aspects of theoretical model and software.

(g) Recently, Bagdasarian (1994) reported new progress on assessing the structural integrity of bridges through vibration monitoring. Recent studies at the University of Connecticut have shown that monitoring a bridge's dynamic characteristics is feasible. Laboratory testing on a bridge model developed a bridge "signature" comprising the bridge's natural frequencies and mode shapes. Changes in the "signature" correspond to changes in the model's structural stiffness. Therefore, these components of the "signature" (the natural frequencies and mode shapes) could be used to evaluate the structural condition of the bridge.

(h) A prototype monitoring system was developed by Vibra-Metrics, Inc., for placement on an actual Connecticut bridge. The monitoring system consists of sixteen accelerometers, two cluster boxes, and a sentry unit that houses a computer.

(i) The accelerometers act as sensors for detecting the bridge's vibrations. They are magnetically attached to the bridge girders and positioned throughout the floor plan of the bridge as shown in Figure B-3.

(j) The signals received by sensors in time domain from the vibrating bridge are transformed into the frequency domain by the monitoring system software. The frequency spectra are imported into the DADiSP program, where they are analyzed to determine the natural frequency peaks for monitoring purposes. Figure B-4 shows the natural frequencies and mode shapes of signals from sensors at different locations. Spectrum clean-up techniques are designed to enhance the appearance of the frequency spectrum. Cleaning a spectrum enables one to identify natural frequencies with less difficulty, thus allowing for the determination of changes in the natural frequencies indicating structural deterioration of the bridge.

c. *Ultrasonic testing method.*

(1) Principle.

(a) Ultrasonic waves are simply vibration waves with a frequency higher than the hearing range of the normal human ear (i.e., 20 kHz). The pioneer work in ultrasonic testing was accomplished by Langevin of France, who experimented with ultrasonic submarine detection methods during World War II. Now, most practical ultrasonic discontinuity detection is carried out with frequencies from 200 kHz to 20 MHz. Ultrasonic waves with 50 MHz or

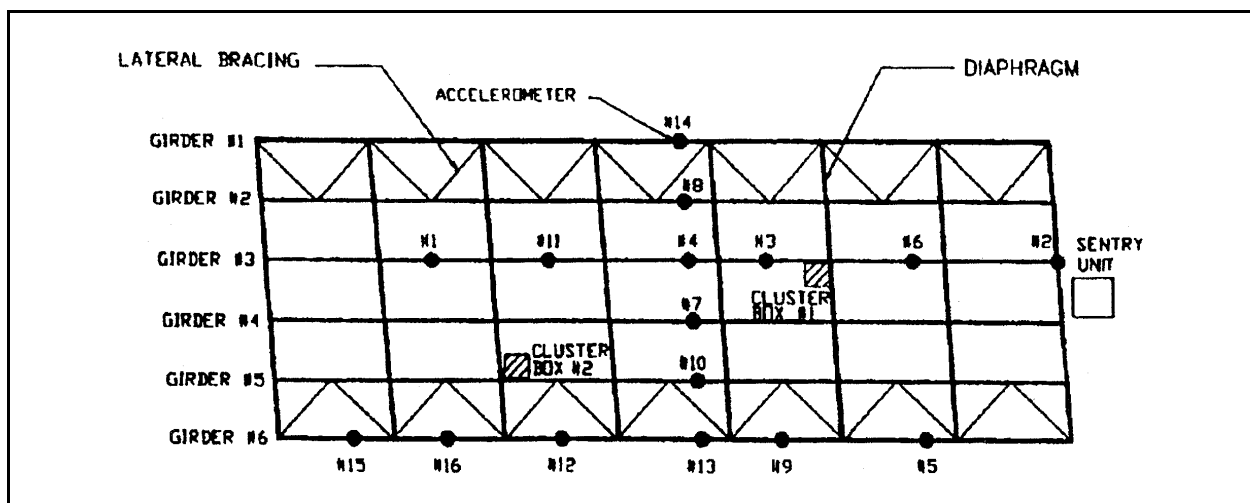


Figure B-3. Bridge floor plan with accelerometer locations

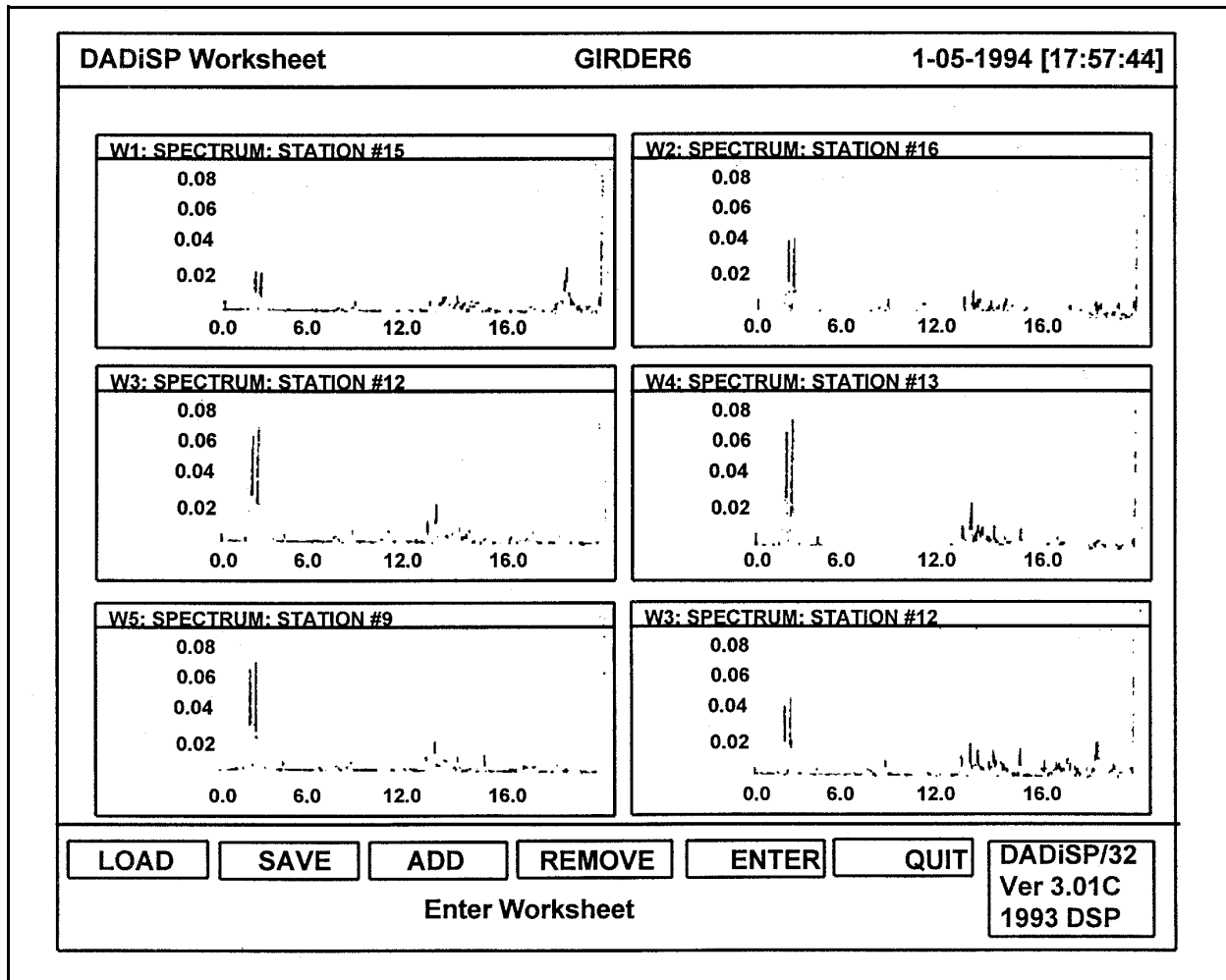
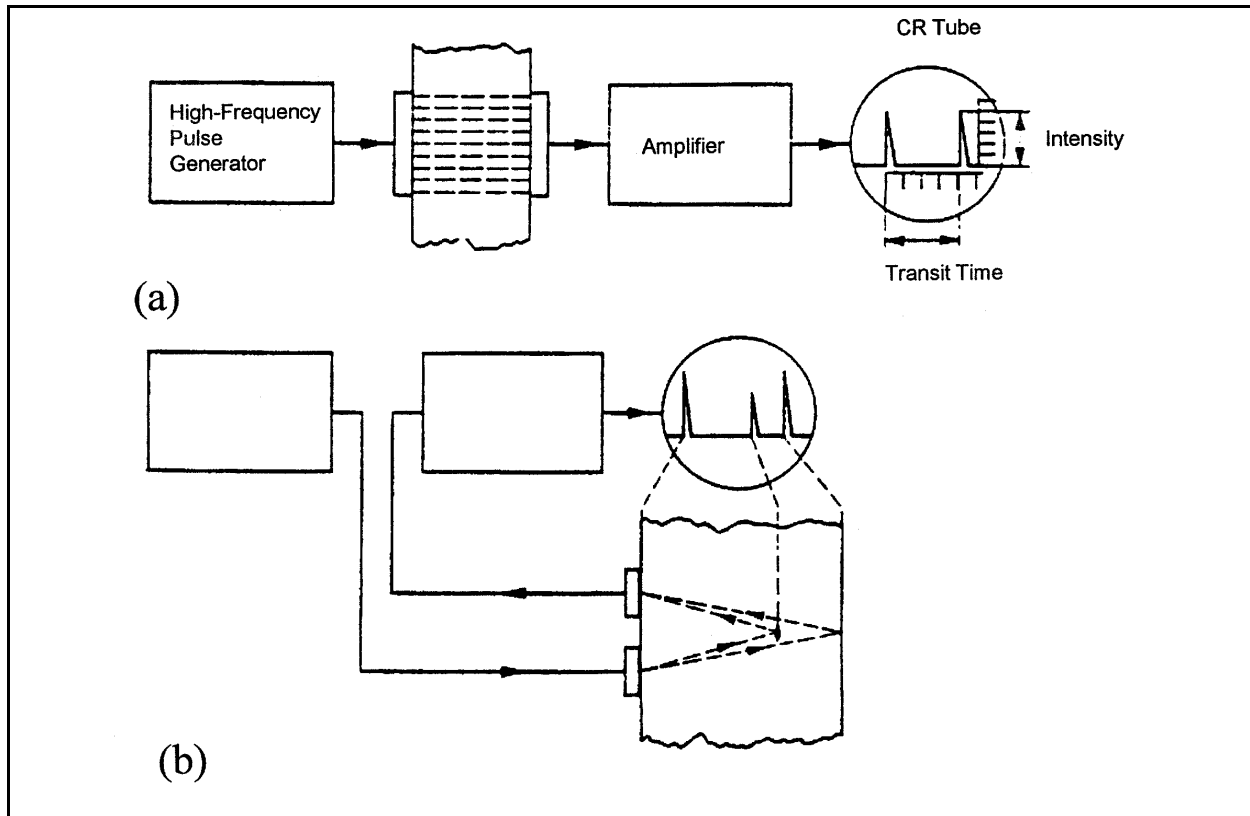


Figure B-4. Typical worksheet

higher frequencies are sometimes used in material property investigations.

(b) Ultrasonic inspection is accomplished by using electronically controlled pulses introduced into a material through a transducer. The ultrasonic energy then travels within the material, finally reaching an outer surface where the ultrasonic waves are received by the same or another ultrasonic transducer. Materials with discontinuities are diagnosed from the characteristic of the received ultrasonic energy. In this method, the wave intensity and the transit time are measured (e.g., on the screen of a CR tube as shown in Figure B-5). Perfect material without defects is assumed in Figure B-5(a), where the first

pulse on the CR tube screen is from the exciting pulse, and the second pulse measures the transit time in the material sample. When a discontinuity exists in the material, the pulse due to the discontinuity reflection can be found, as shown in Figure B-5(b). The intensity of the flow echo is directly related to the discontinuity properties, and the position of the discontinuity echo reflects its locations. Variance in the discontinuity properties of fatigue cracks in bridge beams using ultrasonic methods has been reported by Hearn and Cavallin (1997). In most cases, one ultrasonic transducer (or probe) is used in the inspection. This method is also called A-scan presentation, furnishing a one-dimensional description for a given test point Figure B-6(a).



**Figure B-5. Intensity transit-time or pulse transit-time method, (a) with sound transmission, (b) with reflection**

(c) In the so-called B-scan method, the location (depth) of a discontinuity in a specimen is represented by echo position (usually along the vertical direction) and the amplitude of the discontinuity echo by the brightness, as shown in Figure B-6(b). In the case of two-dimensional (area) scanning of a test piece (e.g., a plate), the test results can be presented by means of a C-scan Figure B-6(c). This method furnishes a top view of the test piece from the scanned surface with plotted flaw projection points.

(d) Some of the advantages of ultrasonic methods are as follows: discontinuities can be detected in metallic and nonmetallic materials; discontinuity distance may be measured from the material surface; discontinuities can be located in very thick materials; only single-surface accessibility is required; both internal and surface discontinuities may be detected; discontinuity imaging is possible, and material properties can be measured.

The ultrasonic technique has rapid testing capabilities, and portable instrumentation is available for field testing. Equipment for automatically recording inspection results is available, and the inspection costs are relatively low.

(e) Conversely, there are some disadvantages of ultrasonic testing: there may be difficulties incoupling energy to rough surface; it may be impractical to inspect complex shapes; flaw imaging is complex; and special scanning systems may be required for inspecting large surfaces.

## (2) Applications.

(a) Computer-controlled multifunctional ultrasonic instruments for detecting discontinuities in materials have been highly developed (Woo and Daniel 1994). These techniques can be used to detect cracks, voids, and other abrupt

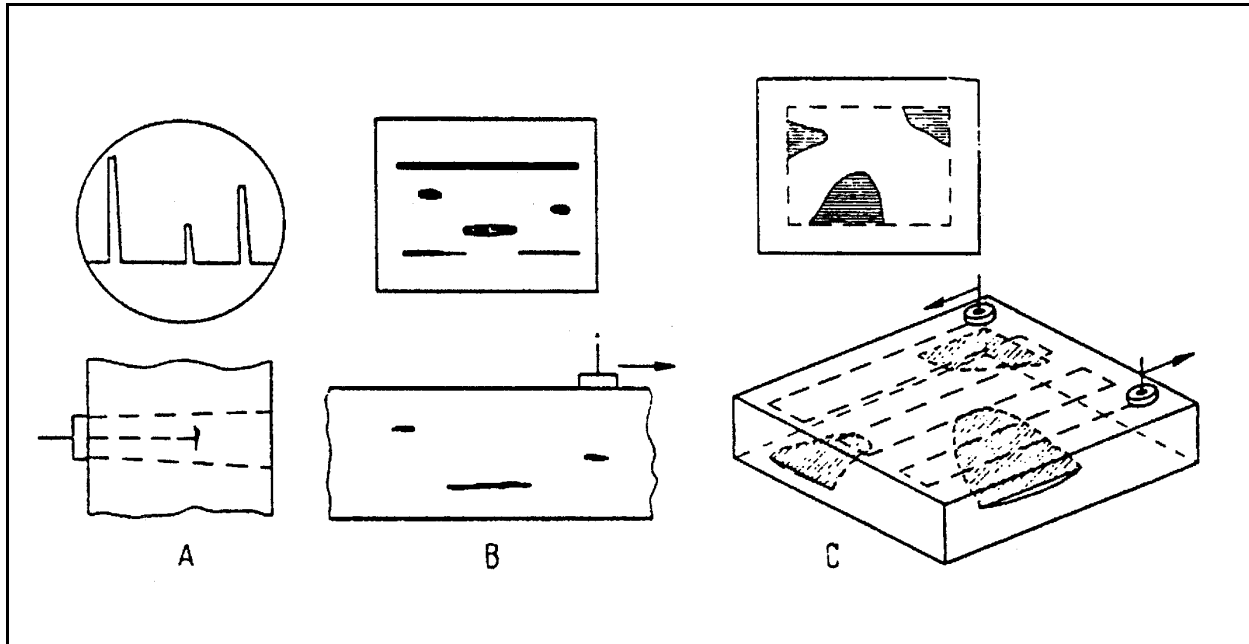


Figure B-6. A-, B-, and C-scan presentation and scanning method

discontinuity or lack of homogeneity in metallic, nonmetallic, and composite materials (Krautkrämer and Krautkrämer 1977, Bray and McBride 1992, Wooh and Daniel 1994, Thavasimuthu et al. 1993, Cruby and Colbrook 1992, and Berger 1992). On-line weld monitoring using ultrasonics is also well developed (Stares et al. 1990; Bull et al. 1995; and Prikhod'ko and Fedorishin 1993).

(b) Major limitations of these techniques involve attenuation characteristics of certain materials, access problems, very tight cracks, and complex geometric configurations. Even with these limitations, ultrasonic discontinuity evaluation technology is very effective when properly applied. Some typical applications are listed in Table B-3.

**Table B-3**  
**Some Sources of Acoustic Emissions**

Raw materials	Adhesive bonds
Weldments	Aircraft
Castings, forging	Spacecraft
Pipe	Nuclear reactors
Seamless tubes	Ships
Railroad wheels, rails, and axles	Bridges

(c) Examples of applications which are related to the structural inspection of bridges include the following:

- **Normal-beam inspection of bars and plates.** One of the most common tests performed with ultrasound is the inspection of structural plates and bars for interior discontinuities and corrosion using a normal-beam and longitudinal-wave probe. These tests are applied to both plain material and fabricated members.

A typical A-scan, digitized RF display of a normal-beam inspection is shown in Figure B-7(a). The test sample is an aluminum bar 76 mm thick. With a sampling rate of 20 MHz and an expansion of 1, the time base is 36  $\mu$ s. The echo occurring at 15.7  $\mu$ s (point A) past the main bang indicates a discontinuity at approximately 49 mm below the probe. The back echo appears at 24  $\mu$ s (point B) beyond the main bang.

The horizontal bar above the discontinuity echo (point A) indicates a gate starting at 17.8  $\mu$ s and 2.95  $\mu$ s in length. One use of a gate is to select a signal for frequency analysis as shown in Figure B-7(b). The output shows the peak power

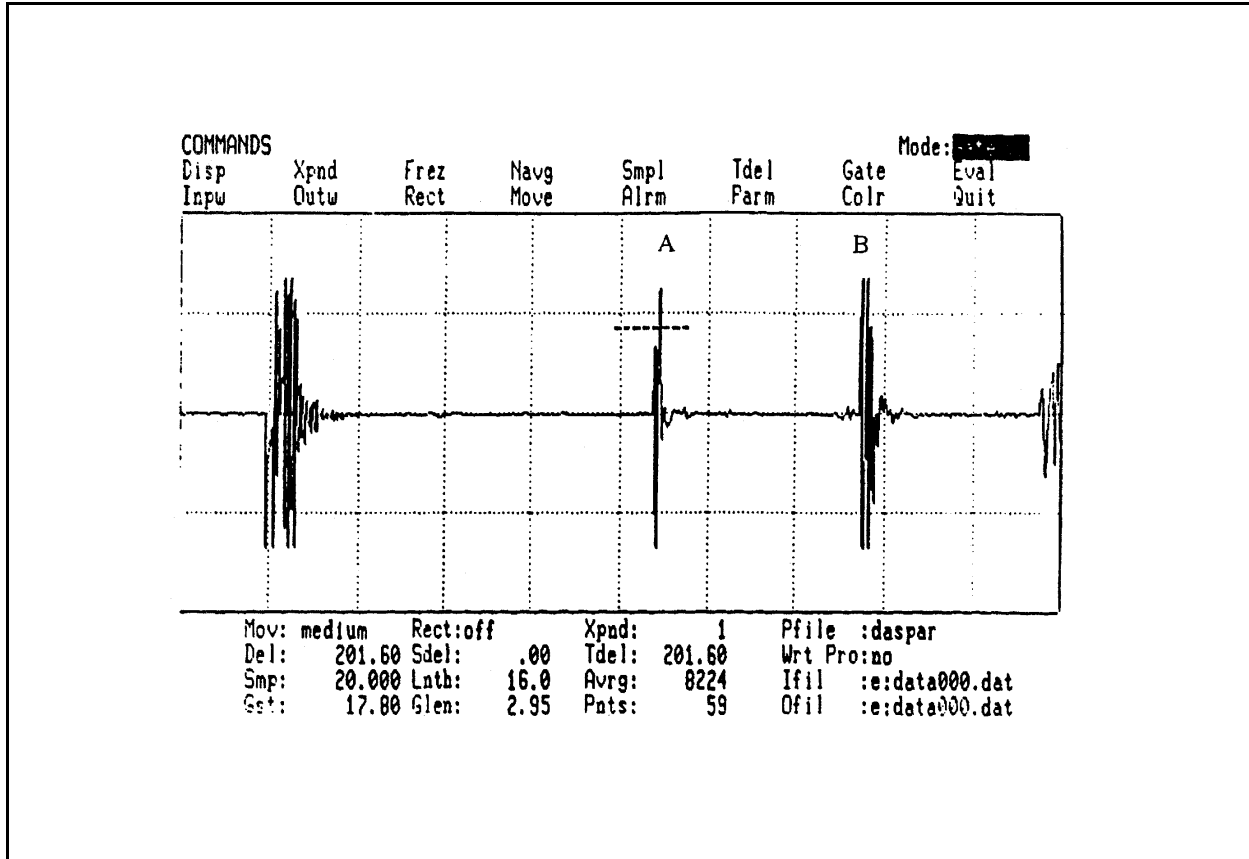


Figure B-7(a). Typical digitized RF display of test of aluminum bar 76 mm (3 in.) thick. Time base is  $3.6 \text{ E-6x/div}$ .

spectrum frequency to be 5 MHz, which agrees with the frequency of the probe. Other information shown in the figure describes additional parameters used in signal analysis (Bray and Stanley 1984).

- **Welded joints.** The following types of manufacturing defects can be detected in welded butt joints using ultrasonics: slag inclusions, pores, lack of fusion (cold shuts), lack of penetration, and cracks. Figure B-8(a) shows the ultrasonic testing of a welded joint with normal longitudinal probes, and Figure B-8(b) illustrates testing of a welded joint with transverse probes. Figure B-9 shows testing of fillet welds.

(3) Inspection of bridges.

(a) The ultrasonic techniques are used to inspect bridge components such as beams, girders, and chords before a bridge is completed. The

allowable discontinuity size in the components is highly restricted during fabrication. However, during shipping, handling, and erection of bridge components, new cracks may grow. Therefore, it is suggested that bridge components should be inspected both during and after construction.

(b) In Japan, ultrasonic testing is utilized for nondestructive in-process evaluation. As a rule, automatic ultrasonic testing inspection is performed for welded chord members. Ultrasonic testing of in-service bridges is time-consuming. To date, no real-time structural damage assessment of bridges is reported.

d. *Acoustic emission method.*

(1) Principle.

(a) Acoustic emission (AE), sometimes called stress wave emission, is a transient mechanical

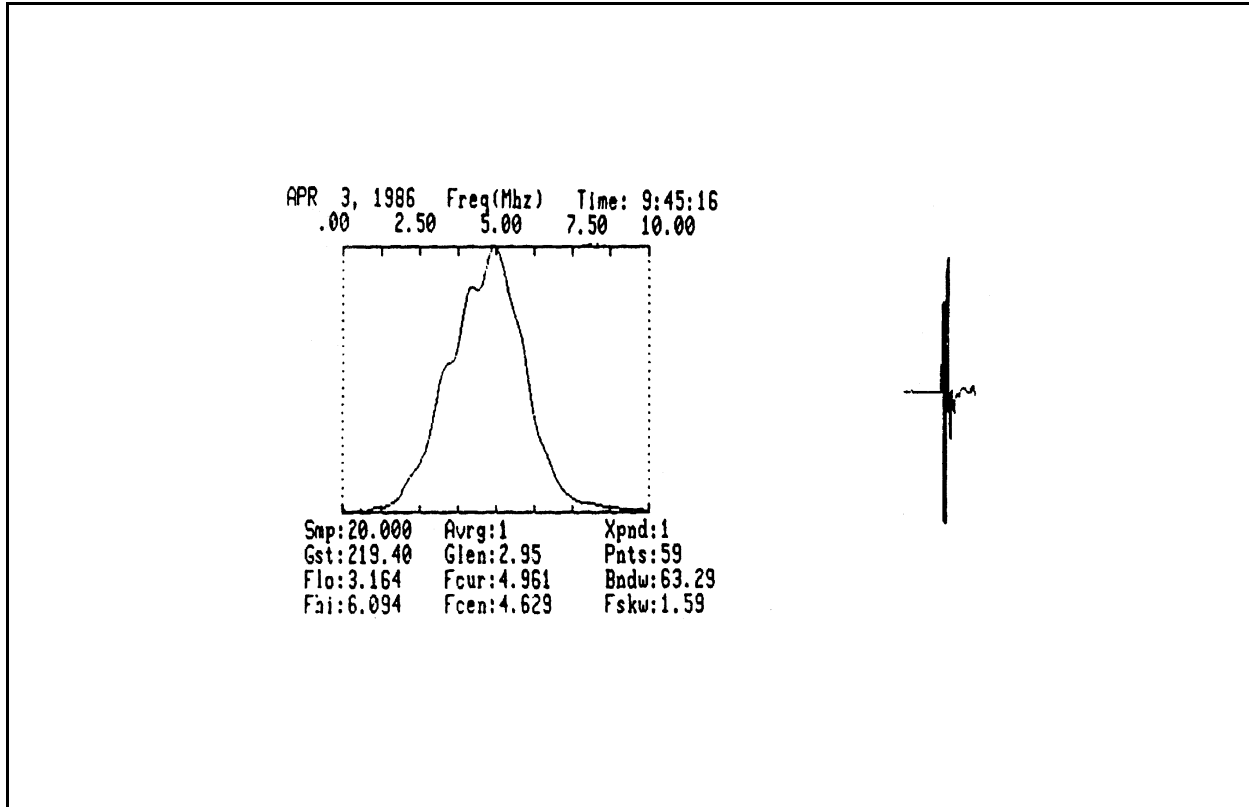


Figure B-7(b). Power spectrum for ultrasonic signal

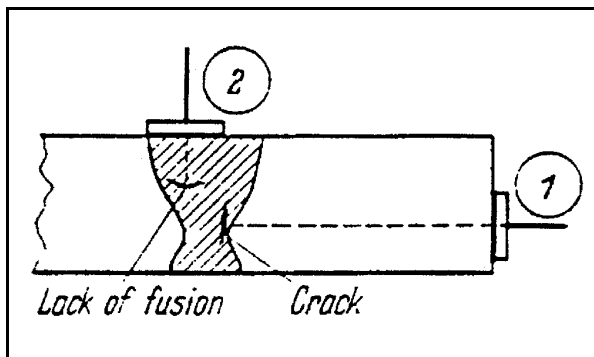


Figure B-8(a). Testing of welded joint with normal probes

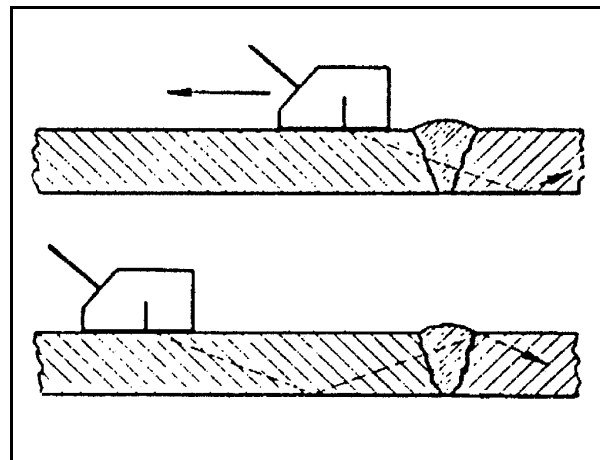


Figure B-8(b). Test of welded joint with zigzag transverse waves

vibration generated by the rapid release of energy from localized sources within materials. Stress or some other stimulus is required to release or generate emissions. Emission energy levels can range from the motion of a few dislocations in metals to that required to cause catastrophic cracking of structures. Some stimuli causing acoustic emissions are given in Table B-4.

(b) Acoustic emission signals cover a wide range of energy levels and frequencies but are usually considered to be of two basic types: burst and continuous. The term *burst* is a qualitative description of emission signals corresponding to

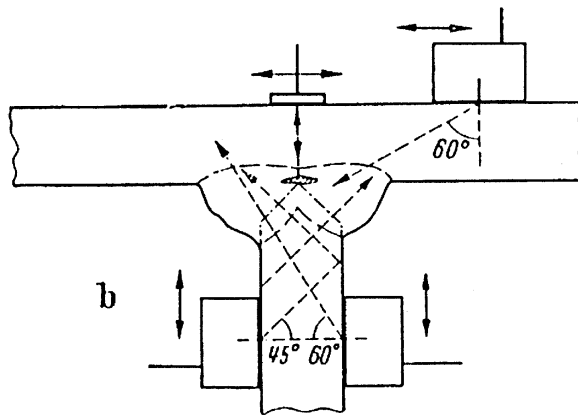
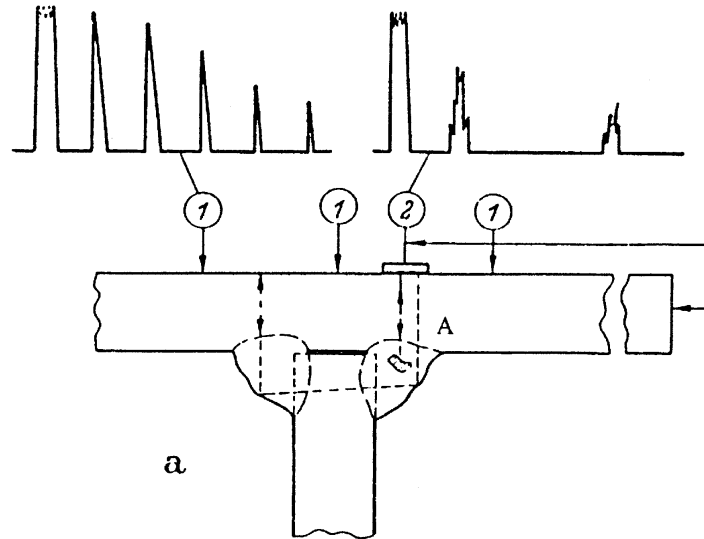


Figure B-9. Testing fillet welds; (a) joint not welded through, (b) joint welded through (K-joint)

**Table 4**  
**Some Sources of Acoustic Emissions**

Crack initiation and growth
Dislocation movements
Twinning
Phase changes
Fracture of brittle inclusions or surface films
Fiber breakage, crazing, and delaminations in composites
Chemical activity

individual emission events. The term *continuous emission* is a qualitative description for an apparently sustained signal level from rapidly occurring emission events. Emission frequencies range from below to well-above the audible range for humans. But most practical AE monitoring is accomplished in the kilohertz or low-megahertz range.

(c) Although emission is characterized as burst or continuous, signals of either type may propagate in any of the standard ultrasonic modes (i.e., shear, longitudinal, or surface waves). Furthermore, a single emission event can generate waves having more than one propagation mode.

(d) A wide range of transducer types has been used to sense acoustic emission from materials, structures, and industrial equipment. The types of AE sensors include accelerometers, piezoelectric transducers, capacitive transducers, optical/laser sensors, microphones, strain gauges, magnetic-strictive sensors, etc.

(e) The most widely used method of quantifying AE signals is the ringdown counting technique, which measures the characteristics of the emitted signal as its amplitude decays. For a typical sinusoidal AE pulse, an amplitude threshold is established for the acceptance of signals, and the number of signals exceeding this threshold is automatically counted by the instrumentation system. Signals crossing the threshold are usually plotted as a function of load, stress, time, or other parameters. They may be plotted as the count rate versus stress, or the plot may be of the total or cumulative count versus the selected parameter. The data presentation techniques are illustrated in Figures B-10 and B-11. The significant parameters used in characterizing acoustic emission

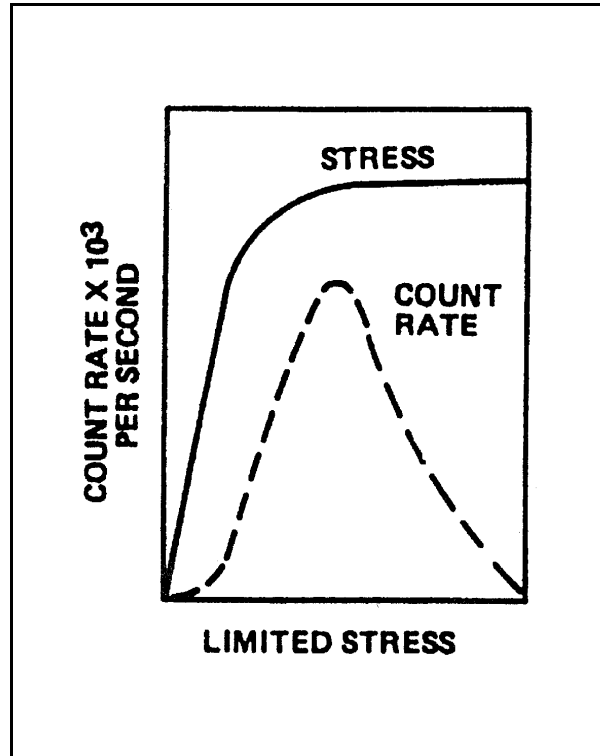


Figure B-10. Generalized count rate versus stress

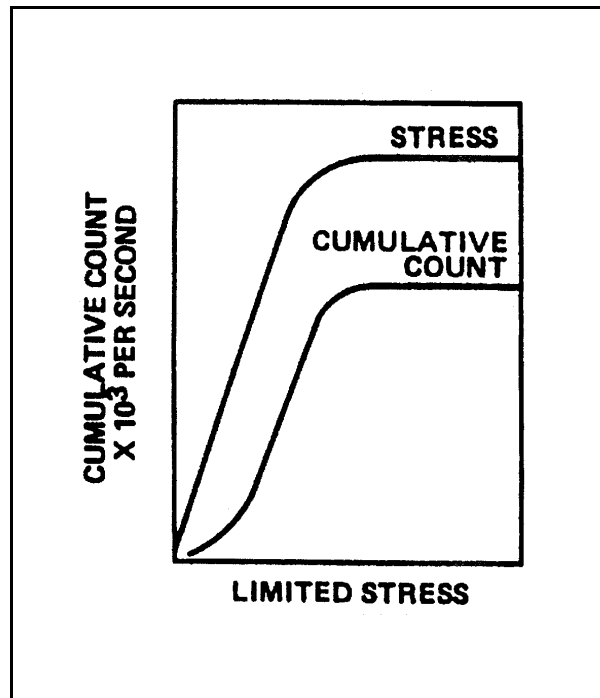


Figure B-11. Generalized cumulative count versus stress

events are peak amplitude, frequency, duration of signal above the selected threshold, number of counts per event, energy, and rise time. Some of these parameters are indicated in Figure B-12. These parameters are related to the various AE sources in different ways. For example, the AE count rate associated with plastic deformation at the tip of a crack may be expressed as (Muravin et al. 1993)

$$N = (ChK_{max}^2/\sigma_y) dl/dn \quad (B-6)$$

where

$C$  = a proportionality factor

$h$  = thickness of the specimen

$K_{max}$  = maximum value of the stress intensity factor

$\sigma_y$  = yield point

$dl/dn$  = growth rate of the crack length for loading cycle

(f) For engineering applications, it is more convenient to find out the relationship of AE count rate with the stress intensity factor range  $\Delta K$ . For fatigue fracture in materials, Morton et al. (1974) and Bassim (1987) present the following equation:

$$N = A (\Delta K)^n \quad (B-7)$$

where  $A$  and  $n$  = experimental constants. This equation is similar to the well-known Paris law of fatigue-crack propagation (Paris et al. 1963):

$$dl/dn = C (\Delta K)^m \quad (B-8)$$

where

$dl/dn$  = crack-growth rate

$C$  and  $m$  = experimental constants

(2) Applications.

(a) The AE method has wide applications. It can be used to monitor changing material

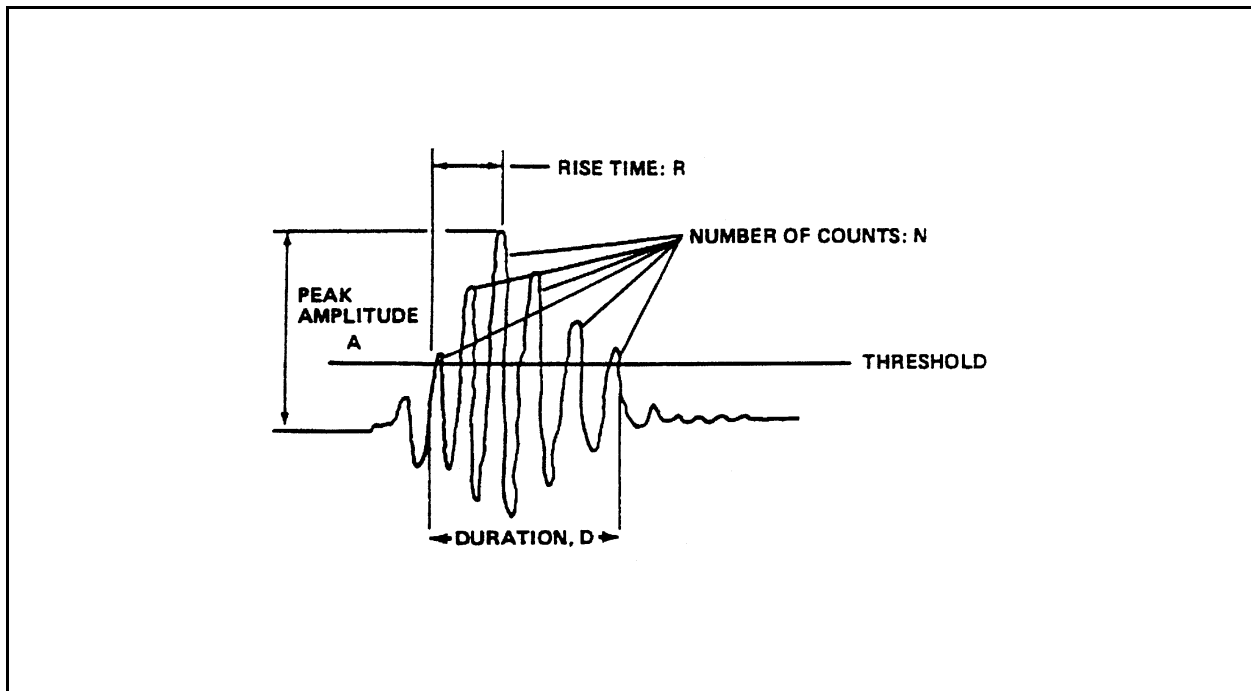


Figure B-12. Parameters used to characterize emission events

conditions in real time and to determine the location of the emission centers as well. Typical applications include on-board or onsite monitoring of aircraft, pressure vessels, tank welds, bridges, and civil engineering structures. In addition, corrosion and bearings in pumps and other rotating machinery such as hydraulic valves can be monitored. Simulated acoustic emission techniques are also useful for monitoring types of composite materials. Some recently reported applications can be found in Ramsamooj (1994), Yuyama et al. (1994), Glaser and Nelson (1992), and Fang and Berkouits (1994).

(b) The advantages of AE are rooted in the basic characteristic where the active defect emits a signal that will find a path to the monitoring sensor location. Since it is a passive technique, no equipment is required to excite a pulse. Further, the received signals may be recorded for remote or delayed analysis and for storage. The requirements for equipment mounted on the monitored structure may be rather small. Other advantages are that AE techniques are highly sensitive to crack growth, and locations of growing cracks can be determined.

(c) Additional advantages are the ability to monitor an entire system at the same time. With remote monitoring, the technique can be used in hostile environments. The item being tested usually can remain in operation during the process, and the entire volume of materials and structures can be inspected at a reasonable cost. It is also suitable for long-term in-service monitoring.

(d) Disadvantages of the technique include the requirement of stress or other stimuli to generate the acoustic emission event. Therefore, stabilized cracks cannot be detected with emission techniques. The size of cracks or other defects cannot be precisely determined. Some materials and certain tempers of other materials are not very emissive and are unsuitable for monitoring. Electrical interference and ambient noise must be filtered out of emission signals. Also, the multiple number of travel paths from the source to the

sensor in complex structures can make signal identification difficult.

(3) Inspection of bridges.

(a) AE techniques were used in the 1970s to monitor some bridges (Pollock and Smith 1972; Hutton and Skorpik 1975). In the 1980s, extensive studies were carried out to use acoustic emission techniques for bridge inspections (Fisher and Wood 1988; Hopwood and Prine 1987; and Green 1988). It was reported that (Hopwood and Prine 1987) an experimental AE device, the Acoustic Emission Weld Monitor (AEWM), has been field tested on six bridges during the study. The device was also used to test three other bridges under separate contracts from state highway agencies. The AEWM was evaluated to determine if it could detect fatigue-crack growth on in-service steel bridges. The device rejects high background noise rates typical of bridges and detects and locates AE activity from known defects such as cracks and subsurface discontinuities. The AEWM functioned properly in every field test situation to which it was applied. The AEWM has demonstrated capability to perform AE tests on in-service bridges. It may also be used to detect hidden discontinuities or assist in making repair decisions concerning detected discontinuities. The AEWM and AE testing have been demonstrated to have the potential for low-cost inspection of critical bridge members.

(b) Some newly accomplished inspections of bridges by the AE techniques are also reported (Hariri 1990, Azmi 1990, Vannoy and Azmi 1991, and Gong et al. 1992). A comprehensive examination of characteristics of acoustic emission signals generated from steel beams (rolled and welded sections) and other steels used in highway bridge structures was made. The effective frequency range for monitoring highway bridges was established. In these inspections, the thickness and surface conditions of bridge components are varied. Crack lengths were measured at the time of data collection, and various acoustic emission parameters were plotted versus the stress intensity

factor of the specimens. It was discovered that acoustic emission signal characteristics for the steel types used in highway bridges are similar although, the signals vary according to the thickness of the material. It was also discovered that the corrosion surface enhances the intensity of the signal, and paint layers do not have a significant effect on the attenuation of the AE signals.

(c) Recent inspection of steel railroad bridges by the AE method is presented by Gong et al. (1992) in which they demonstrate successes using AE to find new cracks, to identify active cracks, to validate the effectiveness of repairs, and to provide damage assessments to assist with repair prioritization.

(d) As given in Equation B-7, the stress intensity factor range  $\Delta K$  for fatigue fracture is highly related to the acoustic count rate  $N$ . The typical relationships among the acoustic count

rate, the crack-growth rate, and  $\Delta K$ , based on laboratory tests of typical bridge steel, are shown in Figure B-13. It can be seen that the count rate increases as a crack grows, and for an active fatigue crack, the count rate presents an increasing slope under constant cyclic loading. This result indicates that a positive slope of the count rate over time during field testing may be used as a means of judging crack severity when compared to similar slopes obtained from laboratory tests on the same material. Table B-5 and Figure B-13 show a method of classifying fatigue cracks in bridge steel into five safety index levels based on the range of structure  $\Delta K$  determined by AE monitoring. This approach has been effectively used in interpreting  $\Delta K$  levels obtained from field monitoring and applying them to the prioritization of crack repair programs.

(e) The Monac multi-channel field AE-monitoring system is currently being used to

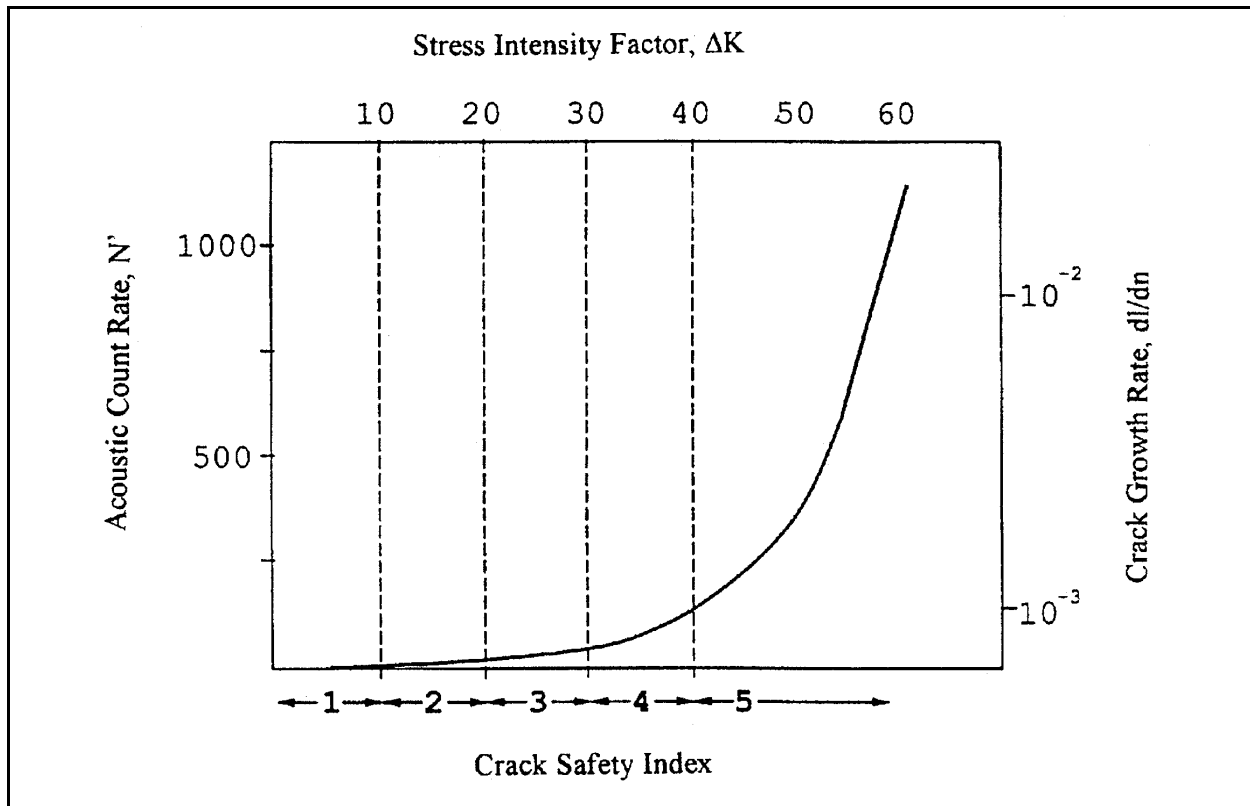


Figure B-13. Typical relationships among the crack safety index, crack-growth rate, count rate, and  $\Delta K$  for bridge steels

**Table B-5**  
**Fatigue-Crack Characterization for Bridge Steels**

Range of $\Delta K$	Crack Safety Index	Crack Description
$0 \leq \Delta K < 10$	1	Minor defect
$10 \leq \Delta K < 20$	2	Slow crack growth
$20 \leq \Delta K < 30$	3	Requires repair
$30 \leq \Delta K < 40$	4	Dangerous
$40 \leq \Delta K$	5	Imminent failure

monitor 36 bridges under normal loading conditions. The system consists of surveillance units and an IBM PC control unit as shown in the Figure B-14 block diagram. A line driver and receiver are located next to each acoustic transducer to ensure the fidelity of weak acoustic signals after transmission over long cables. The monitoring distance can be up to 460 m (1,509 ft). All bridges tested utilized standard piezoelectric transducers with resonant frequencies of 200 kHz.

(f) In total, 353 locations have been monitored on 36 railroad bridges over three years of testing. Each location was monitored continuously from 4 to 10 days, during which time about 40 trains passed over each bridge. Table B-6 gives the results of this monitoring which located 116 active cracks; among them 14 cracks had a safety index of 3 and only one crack had a safety index of 4. No crack had a safety index greater than 4.

(g) Cracks were often found at the webs of floor beams near the upper corners of the connection angle with a stringer. In most cases, such cracks had initiated because of the bending moment on the stringer end. AE monitoring indicated that two such cracks had a safety index of 2. Many fatigue cracks were also found on the top flanges of stringers.

(h) It was found that welds were always the most crack-sensitive areas, possibly due to residual stresses and stress concentrations. Therefore, current recommendations for bridge maintenance and repair favor bolting and riveting rather than welding (Fisher et al. 1990).

*e. Optical fiber method.*

(1) Principle.

(a) Like an elastic waveguide, a fiber can guide high frequency electromagnetic waves (optical waves) (Kao 1988 and Katsuyana and Matsumura 1989). In a perfect symmetric and homogeneous fiber waveguide, the waveforms of guided modes propagate undisturbed along the waveguide axis. However, a deformation or inhomogeneity in fiber geometry may cause coupling among different modes, resulting in power transfer. In particular, the guided modes may be coupled to radiation modes, which are not confined. The resulting power transfer represents an attenuation. Similarly, any deformation of material attaching the fiber can also give rise to the mode coupling and guided wave attenuation. Therefore, the received optical wave in fiber can be intensity modulated by the deformation of the outside material. The guided wave can also be phase modulated due to the change of its geometric form which is caused by the strain or deformation on the outside material.

(b) An optical fiber embedded in structures will deform together with the structure. The light passing through the optical fiber can be modulated either in intensity or in phase. This effect has been implemented in a form called "Smart Strain." By analyzing the changes of light intensity or phase transmitted by embedded fiber, dangerous strain levels in the structure as well as failure of material may be detected. A system of such optical fiber sensors embedded in a structure could act as the "nervous system" of the structure.

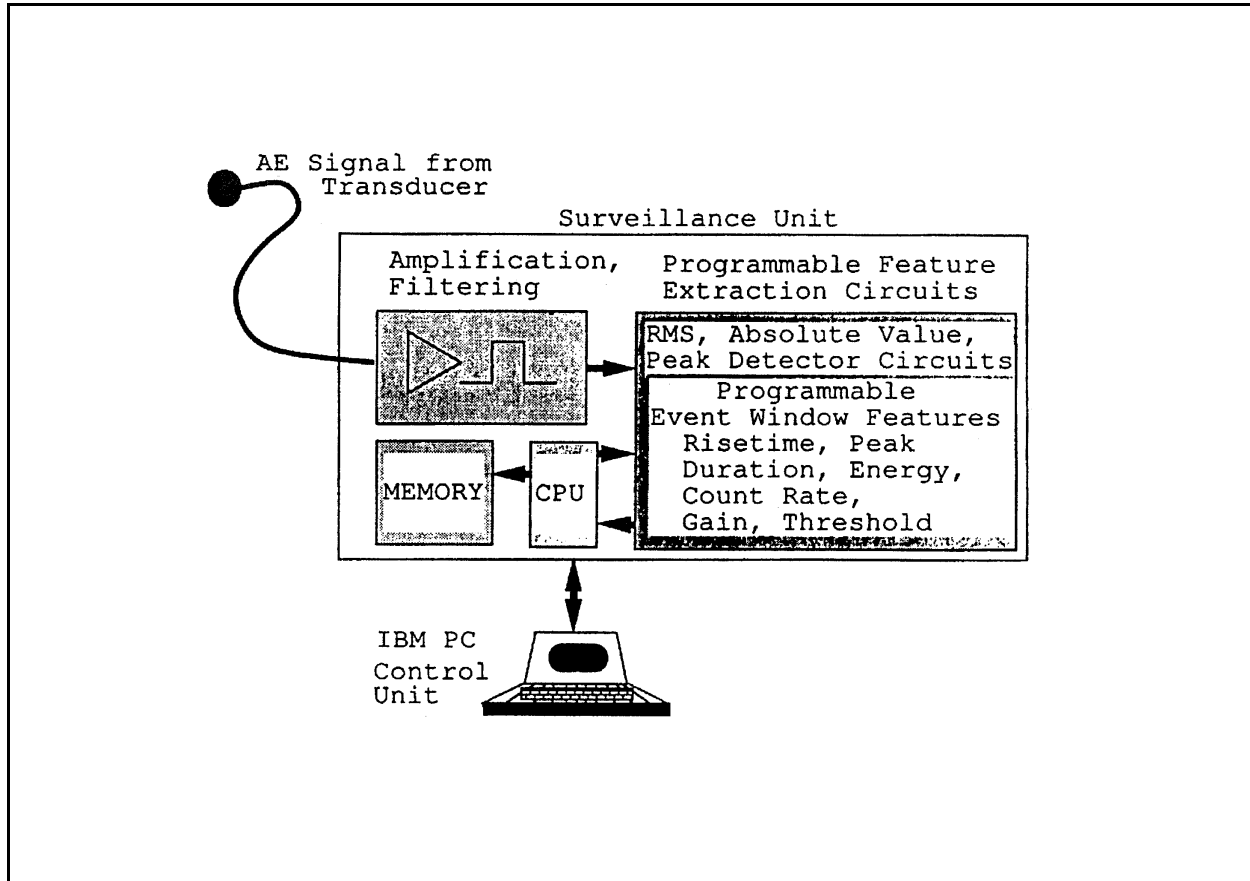


Figure B-14. Block diagram of the Monac acoustic monitoring system. RMS = root mean square

(c) A typical experimental arrangement for an optical fiber sensor is shown in Figure B-15 (Brennan 1988). The output of a laser diode was used in the input into the optical system which is configured as a polariscope. The circularly polarized light output from the combination of polarized laser output and quarterwave retarder is injected into the optical fiber. Strain induced by beam deformation in the fiber will produce a change in the polarization state at the output. This is measured by the second polarizer acting as an analyzer and the photo-diode. The retardation between the two principle polarization axes is seen as an intensity variation as measured by the photo-diode.

(d) Figure B-16 illustrates another example of optic fiber sensor (Sharma et al. 1981). This is similar to the two-arm interferometer. The fiber numbered 5 in Figure B-16, is subjected to the

external influence, but the fiber numbered 4 is isolated. Any change of the light phase in fiber number 5 will result in the interference fringe displacement. The advantages of optical fiber include its small size, light weight, faster data speed, immunity from electromagnetic induction, positioning, and lower cost.

(2) Applications. Optical fiber sensors have been widely investigated (Asawa et al. 1982; Marvin and Ives 1984; Lapp et al. 1988; Maria et al. 1989). A special conference on fiber optic smart structures and skins was held with more than thirty papers presented at the International Society for Optical Engineering (1988). Following is a brief introduction of some applications of the optical fiber sensors.

- **Mapping strain field.** Optical fiber sensors can be used to provide evaluation of the

**Table B-6**  
**Results of Railroad Bridge Monitoring**

Bridge Number	Bridge Type	Number of Monitoring Locations	Number of Active Cracks	Crack Safety Index				
				1	2	3	4	5
1	TTS	8	2	1	1			
2	TPGV	4	1		1			
3	TPG	6	3	1	1	1		
4	DPG/TPG	7	2		2			
5	TPG	6	0					
6	TTS/TT	8	3	2	1			
7	TT/TPG/TTS	8	1		1			
8	DPG/PYT	7	1		1			
9	TPG/TT	5	0					
10	DPG	5	1		1			
11	TT/DT/DPG	8	3		3			
12	TPG	6	4	1	3			
13	DPG/BM/DPGV	8	1		1			
14	DPG/DT	8	3	2	1			
15	DT/TT	8	6	1	5			
16	DPG/TPG	6	4	3	1			
17	DT	15	3	1	2			
18	TT	13	2		1	1		
19	TT	134	46	23	19	4		
20	TT	12	6	2	4			
21	DT	5	0					
22	TT	6	0					
23	TT	5	2	2				
24	DPG	6	3		3			
25	TT	8	2	2				
26	DPG	12	4	2		2		
27	DPGV	2	1			1		
28	DPGV	2	2		1	1		
29	DPG	3	1		1			
30	DPGV	2	0					
31	DT	6	1		1			
32	DPGV	2	0					
33	DPGV	3	2		1		1	
34	DPGV	3	2		1	1		
35	DPG	2	1			1		
36	DPG	4	3		1	2		

Bridge types: TTS = through-truss swing, TPG = through-plate girder, PYT = pony truss, DT = deck truss, TPGV = through-plate girder viaduct, TT = through-truss, DPG = deck-plate girder, and BM = beam.

state of strain in a structure, i.e., to map the strain field in real time (Measures et al. 1988). The reconstruction of the strain field may be achieved by using the information obtained from the field along a finite number of distinct paths (Figure B-17(a)). This is similar to the reconstruction problem in topography, where the inverse transform is used to obtain the scalar field distribution. The reconstruction of the strain field may also be made by using point fiber optic sensors (Figure B-17(b)).

● **Flight control and damage assessment.**

The fiber optic system composed of a network of embedded sensors may be used to measure the location and extent of damage that may occur during flight, as well as structural integrity prior to take off (Udd 1988). This system could be used in combination with the flight control system to ensure that the aircraft readjusts into a safe flight envelope. The sensors could also be used to measure such parameters as engine temperature, shock position, structural loading, and temperature and pressure distributions augmenting the flight

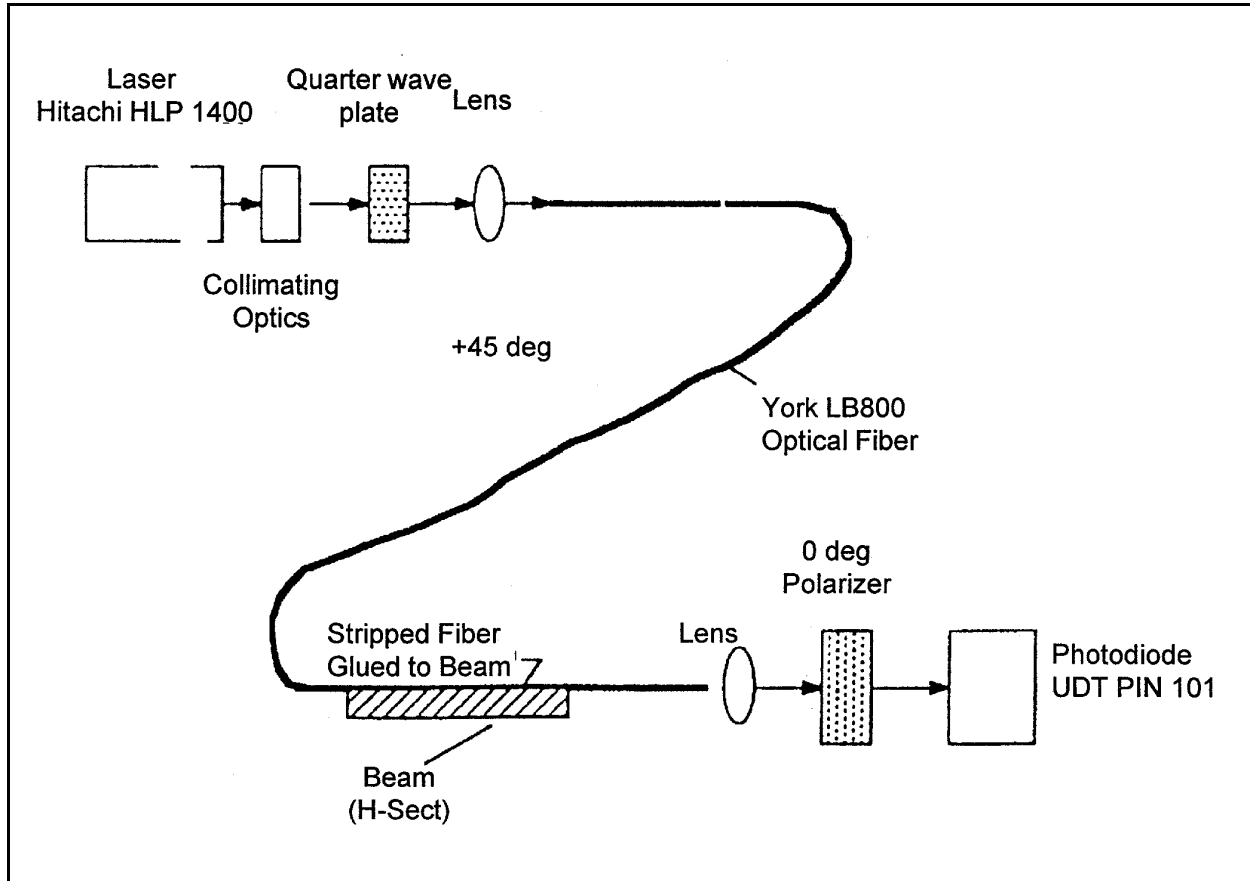


Figure B-15. Optical arrangement

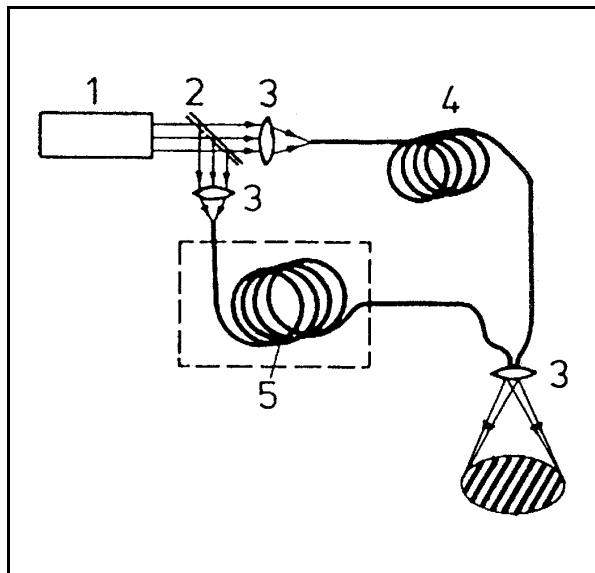
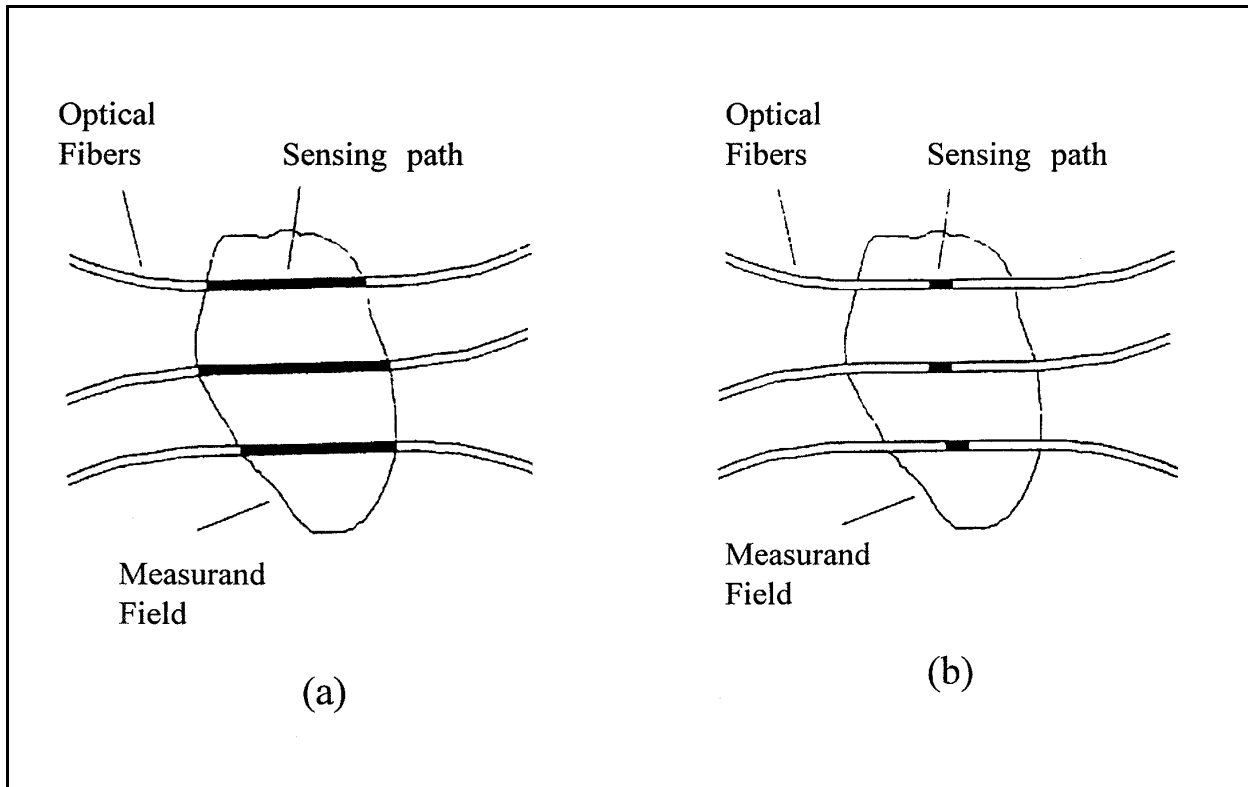


Figure B-16. Illustration of the two-arm interferometer

control system. This concept could be applied to measuring the location and extent of damage to an in-service bridge.

- Vehicle detection and vehicle health monitoring.** The vehicle detection and vehicle health monitoring system requires the installation of 55-cm-long sensing elements on roadways (Tardy et al. 1989). To prevent sensor damage, cable elements are laid into grooves made in the roadway. The laying process consists of placing epoxy resin at the bottom of the groove, installing the sensor cable, then filling the groove with elastomer. Different groove depths have been made. A reflective coating on the end face of the sensor fiber allows the polarization effect to be interrogated by a single fiber with Y coupler. When a vehicle passes over the sensor, a signature of characteristics is developed. The first fringe



**Figure B-17. Reconstruction of the strain field: (a) integrating fiber optic sensors traversing a measured field, (b) using point fiber optic sensors**

shift corresponds to the increased loading created by the vehicle. A continuous signal indicates a quasistatic pressure, while the second fringe shift corresponds to the escape of the vehicle from the sensor. The weight and speed of a moving vehicle may be identified from the fringe number.

- **Concrete structure testing.** In one example, 14-cm-long fiber-optic sensing elements have been embedded in concrete test pieces to determine their response to external pressure (Tardy et al. 1989). Before placing the sensors in concrete, the ribbons outside the sensor are covered with epoxy resin and sand as shown in Figure B-18. These new sensors have been tested in a simple compressive test using a polarimetric apparatus. First readings indicate a sensitivity loss and fringe visibility reduction at the output end of the fiber. The high value of the hardening stress is due to the shrinking phenomenon of concrete. Sensor desensitization is accomplished by loading

the test-piece in a perpendicular plane to that of the ribbons. The observation sensor response is shown in Figure B-19, where the stress axis origin corresponds to the hardening pre-load. The fringe numbers, which are related to the phase change of the propagating light in the optical fiber versus pressure, are in agreement with the theoretical values. If fiber optic sensors are properly embedded in critical parts of bridges, they may be used for structural damage monitoring and structure integrity assessment.

### **B-3. Summary**

*a.* A review of state-of-the-art techniques for real-time damage assessment of bridge structures is provided. Of these methods reviewed, the vibration dynamic and AE techniques have been used in the real-time structural damage assessment of in-service bridges on public roads. These two methods have different physical bases.

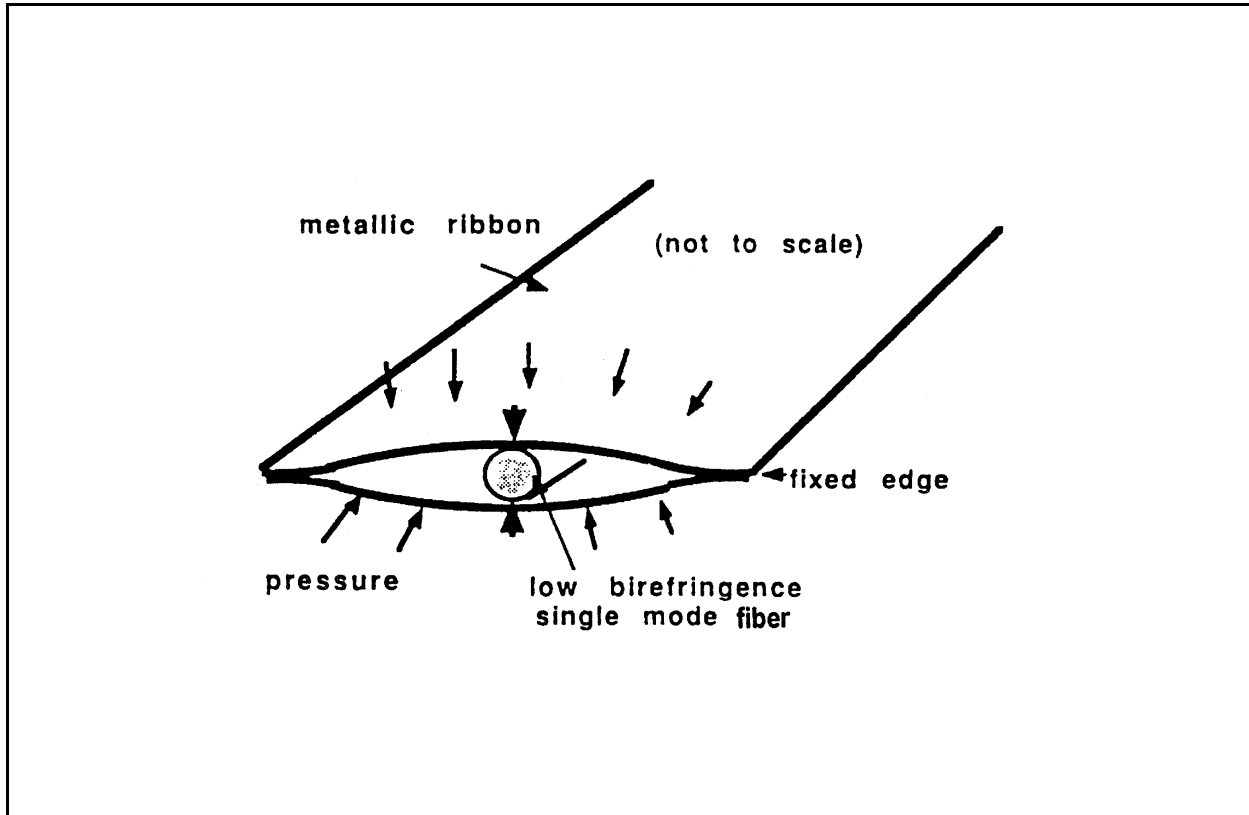


Figure B-18. Sensing structure

*b.* Every bridge has its own natural vibration (or resonance) frequencies, which are related to the materials, structural geometry, and integrity of the bridge. If some components of the bridge are damaged, the resonance frequencies and mode shapes will change. The bridge signature can be used to evaluate the bridge integrity. If cracking occurs on a bridge, acoustic emission signals are emitted. AE techniques have been used for fatigue-crack detection of bridges. The greatest advantage of AE monitoring over the other NDE methods is its ability to detect active cracks and to classify the severity of crack damage.

*c.* Although there are no published papers on the use of optic-fibers to detect bridge damage, optic fiber smart sensors have great potential for monitoring damage incurred in bridge members. All of the methods discussed are on the “cutting-edge” of technology for use in assessing bridge damage. Experimentation of these methods in

real-time bridge damage assessment is still under investigation.

(1) Each critical component of a bridge should be inspected by applying the most appropriate NDE technology (e.g., visual, eddy current, liquid penetrant, magnetic particle, ultrasonic testing, or radiographic inspection) to discover any defects in the components. Members in tension, localized areas around stress concentrations, and areas where a three-dimensional state of stress or high constraint occurs should be considered in the inspection plan.

(2) The vibration dynamic method can be effectively used to make real-time damage assessment of bridge integrity. Each bridge has a special “signature” including resonance frequencies and mode shapes. Some lower resonance frequencies are simulated easier, since they have large vibration amplitude and are

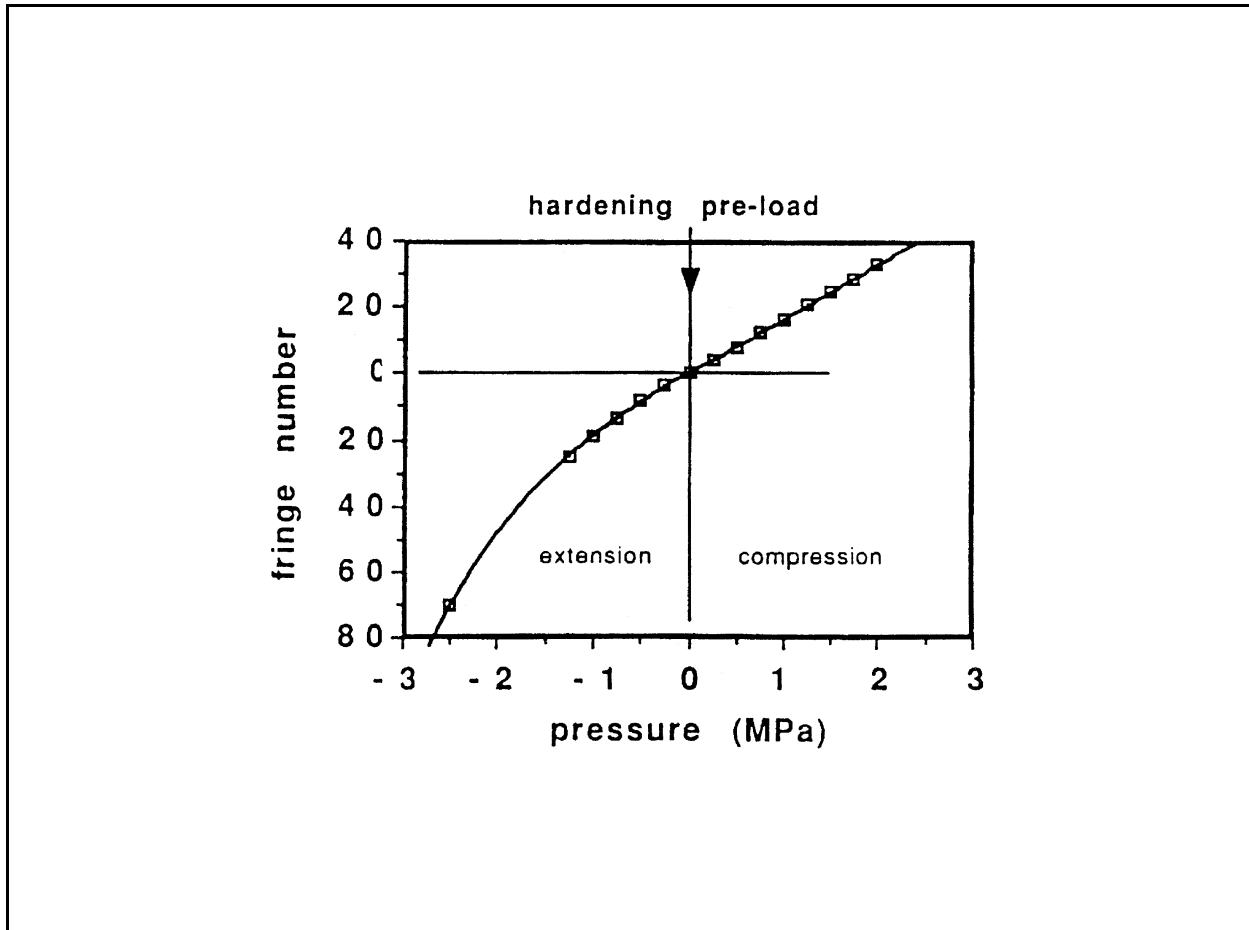


Figure B-19. Experimental response from sensor embedded in concrete

separated from other resonance frequencies. Computer simulations or bridge models may be useful in determining the best location to place transducers to sense the vibration of signals.

(3) AE techniques have engaged the interest of many scientists and engineers in real-time bridge damage assessment. AE signals are developed during crack growth and can be monitored on a real-time sources to the sensor, the signal identification can be difficult. A combination of AE with the vibration or ultrasonic technique may be necessary to completely evaluate a bridge.

(4) The optic fiber method has been widely used to inspect aeronautical facilities. It has not been extensively used for nondestructive evaluation of civil structures such as bridges and buildings. Several advantages (e.g., its small size,

faster data speed, and low cost) of the optic fiber method are attractive for bridge inspection. Application of this method to a bridge would require tightly binding optic fibers to the critical bridge members and monitoring the change of optical intensity or phase at the output end.

*d.* A new application of fiber optics is in crack imaging. It is reported that fiber optical equipment can be used to provide clear and high resolution images of remote cracks contained within critical members (Wilson 1983). This equipment is reported to be easy to handle and operate. Fiber optic techniques have traditionally been applied to the inspection of machined parts on mechanical assemblies, but may also be applicable to the real-time inspection of small areas on critical structural members of a bridge.